Institutionen för systemteknik
Department of Electrical Engineering

Examensarbete

Evaluation of Position Sensing Techniques for an Unmanned Aerial Vehicle.

Examensarbete utfört i Reglerteknik
vid Tekniska högskolan i Linköping
av

Martin Alkeryd

LITH-ISY-EX--06/3790--SE

Linköping 2006

Department of Electrical Engineering
Linköpings universitet
SE-581 83 Linköping, Sweden

Linköpings tekniska högskola
Linköpings universitet
581 83 Linköping

Evaluation of Position Sensing Techniques for an Unmanned Aerial Vehicle.

Examensarbete utfört i Reglerteknik
vid Tekniska högskolan i Linköping
av

Martin Alkeryd

LITH-ISY-EX--06/3790--SE

Handledare: **Johanna Wallén, MSc**
ISY, Linköpings tekniska högskola
Jan-Erik Strömberg, PhD
DST Control AB

Examinator: **Prof. Svante Gunnarsson**
ISY, Linköpings tekniska högskola

Linköping, 31 March, 2006

Avdelning, Institution
Division, Department

Division of Automatic Control
Department of Electrical Engineering
Linköpings universitet
S-581 83 Linköping, Sweden

Datum
Date

2006-03-31

Språk
Language

☐ Svenska/Swedish
☒ Engelska/English
☐ _____

Rapporttyp
Report category

☐ Licentiatavhandling
☒ Examensarbete
☐ C-uppsats
☐ D-uppsats
☐ Övrig rapport
☐ _____

ISBN
—

ISRN
LITH-ISY-EX--06/3790--SE

Serietitel och serienummer **ISSN**
Title of series, numbering —

URL för elektronisk version
http://www.ep.liu.se

Titel
Title

Utvärdering av positionsbestämningstekniker för en obemannad flygande farkost (UAV).

Evaluation of Position Sensing Techniques for an Unmanned Aerial Vehicle.

Författare
Author

Martin Alkeryd

Sammanfattning
Abstract

The use of Unmanned Aerial Vehicles (UAVs) has rapidly increased over the last years. This has been possible mainly due to the increased computing power of microcontrollers and computers. An UAV can be used in both civilian and military areas, for example surveillance and intelligence. The UAV concerned in this master's thesis is a prototype and is currently being developed at DST Control AB in Linköping.

With the use of UAVs, the need for a positioning and navigation system arises. Inertial sensors can often give a good position estimation, however, they need continuous calibration due to error build-up and drift in gyros. An external reference is needed to correct for this drift and other errors. The positioning system investigated in this master's thesis is supposed to work in an area defined by an inverted cone with the height of 25 m and a diameter of 10 m.

A comparison of different techniques suitable for position sensing has been performed. These techniques include the following: a radio method based on the Instrument Landing System (ILS), an optical method using a Position Sensing Detector (PSD), an optical method using the Indoor GPS system, a distance measurement method with ultrasound and also a discussion of the Global Positioning System (GPS).

An evaluation system has been built using the PSD sensor and tests have been performed to evaluate its possibilities for positioning. An accuracy in the order of a few millimetres have been achieved in position estimation with the evaluation system.

Nyckelord
Keywords

UAV, Unmanned Aerial Vehicle, positioning, PSD, trilateration, GPS, PSD, Position Sensing Detector, ILS

Abstract

The use of Unmanned Aerial Vehicles (UAVs) has rapidly increased over the last years. This has been possible mainly due to the increased computing power of microcontrollers and computers. An UAV can be used in both civilian and military areas, for example surveillance and intelligence. The UAV concerned in this master's thesis is a prototype and is currently being developed at DST Control AB in Linköping.

With the use of UAVs, the need for a positioning and navigation system arises. Inertial sensors can often give a good position estimation, however, they need continuous calibration due to error build-up and drift in gyros. An external reference is needed to correct for this drift and other errors. The positioning system investigated in this master's thesis is supposed to work in an area defined by an inverted cone with the height of 25 m and a diameter of 10 m.

A comparison of different techniques suitable for position sensing has been performed. These techniques include the following: a radio method based on the Instrument Landing System (ILS), an optical method using a Position Sensing Detector (PSD), an optical method using the Indoor GPS system, a distance measurement method with ultrasound and also a discussion of the Global Positioning System (GPS).

An evaluation system has been built using the PSD sensor and tests have been performed to evaluate its possibilities for positioning. An accuracy in the order of a few millimetres have been achieved in position estimation with the evaluation system.

Acknowledgements

During the work of this master's thesis many people have been very helpful. To begin with I would like thank my supervisor Jan-Erik Strömberg and the people at DST Control. Thanks for an interesting master's thesis project and good advices. Thanks also to the neighbour companies CybAero AB and Impact Coatings AB for the nice atmosphere.

A big thanks also to my examiner Svante Gunnarsson and university supervisor Johanna Wallén, for quick answers to my questions and valuable comments on the report.

Thanks to my opponent Mattias Eriksson for the comments on my work and my report.

I have received valuable advice regarding electronics and microcontrollers from Erik Alfredsson.

Thanks also to my father, Gunnar Alkeryd, for good ideas and for providing the slide projector.

Anders Lundgren at SiTek AB has given many good advices regarding PSDs.

Park Air Systems has been helpful with discussions of ILS and positioning systems.

Martin Alkeryd
Linköping, spring 2006

This document was prepared using LaTeX on an Apple PowerBook G4. The figures were produced using Dia (from `http://www.gnome.org/projects/dia`) and the plots were produced using Matlab (from Math Works, Inc.).

Contents

Chapter 1

Introduction

1.1 Background

As computers and microcontrollers have become increasingly powerful over the last decades, their areas of use have quickly grown. Today microcontrollers can be found almost everywhere around us: in cars, washing machines, airplanes and mobile phones. For example a modern car contains more than twenty different microcontrollers, doing everything from engine control, controlling the ABS-system and airbag to playing the drivers favourite CD. Modern military fighter planes take the technology one step further and are even built aerodynamically unstable and require the use of an advanced control system to fly properly. The result is flying performances that cannot be achieved with a conventional aircraft. To be able to use a computer-based control system, requirements of reliable actuators arise. The conventional method of using mechanical actuator and controls from the pilot of an airplane or the driver of a car becomes more and more impossible as the microcontrollers take over some of the driving or flying.

Fly-by-wire and Autonomity

The term drive-/fly-by-wire means that there is no actual mechanical connection between for example the steering wheel of a car and the wheels. A sensor interprets the driver's movements of the steering wheel and one or more microcontrollers calculate and perform the required adjustments of the wheels.

The step of completely replacing the pilot or driver is not very big when a drive-/fly-by-wire system exists, and in many situations a computer can do a similar (or even better) job: a computer does not get tired, bored or loses concentration after hours and hours of monotonous tasks.

Unmanned Aerial Vehicles are of good use in hazardous situations when there may be danger for the life of for example the pilot and the crew of an aircraft. The use of UAVs has increased over the last few years, however there is still much research remaining to be done in the field of UAVs. Areas of use include both civilian and military applications, for example surveillance, reconnaissance,

tactical analysis, crisis management, power line inspection, and several more.

Bombus

The UAV concerned in this master's thesis project is a prototype and is currently being developed at DST Control AB under the working name "Bombus". Bombus is the Latin name for some species of bumblebees. The purpose of the Bombus project is to develop a low weight, cost efficient, robust and easy to use unmanned aerial vehicle. The vehicle is based on a ducted-fan design and has a weight of approximately 5 kg. The purpose of Bombus is to provide a complement to today's expensive and relatively large UAVs, hence low cost and low weight are two key parameters during design and choice of technology.

The Bombus UAV is intended to hover at a stationary point in the air, while for example having a camera directed towards a target. The UAV is intended to work both outdoor and indoor. Keeping the desired position in a real outdoor environment is however not trivial. Different kind of disturbances such as changing winds from different directions and inaccuracy in the control loop and actuators may cause the vehicle to deviate from the desired position. Although the on-board control system is likely to include gyros and accelerometers for measurement of those disturbances, an external reference system is needed to correct for gyro drift and error build-up during accelerometer integration.

The work done in this master's thesis is intended to evaluate the potential of different technologies for ground-based position estimation and implement and test one of them.

1.2 The Vehicle

This section will give a brief description of the vehicle, its design and different components.

Overview

In Figure 1.1 a 3D-model of the Bombus UAV is shown. The vehicle consists of an electrical engine driving a propeller (a so-called ducted fan). Below the propeller the "guiding vanes" (not visible) are mounted with the purpose of neutralising rotation caused by the propeller, and furthest down are the rudders. The guiding vanes can be seen in Figure 1.2.

Ducted Fan

The use of a ducted fan is a method to improve the lift force created from a propeller, and is done by putting a "tube" outside the propeller. The main advantage is that the duct ("tube") stops air from "leaking out" on the sides. All air in the duct is forced downwards by the propeller and the duct. In Figure 1.1 the duct of the Bombus vehicle can be seen. Another advantage is that the duct protects the propeller from mechanical damage when operating in an environment with

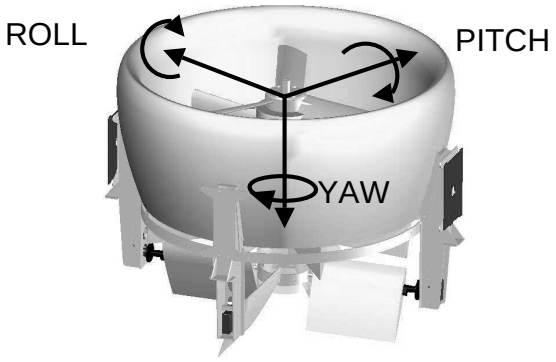

Figure 1.1. A 3D-model of the Bombus UAV.

obstacles. A possible collision with an obstacle may be just a "bump" instead of a destroyed propeller and resulting crash.

Rudders

The vehicle has four rudders, which are supposed to create torque to manoeuvre the vehicle in the air. Initial tests and simulations in [6] have shown that the forces from the original rudders (shown in Figure 1.1) may not be enough to orientate the vehicle in a desired way, especially not when there are wind disturbances present. An approach with "twin rudders" has been tested in [8] and possibly this will solve the problem. The twin rudders are constructed by simply putting two parallel rudders at each rudder position. In Figure 1.1 the original design with single rudders is shown.

Guiding Vanes

The guiding vanes consist of several fixed "rudders" mounted in a circular way as shown in Figure 1.2. The rotating propeller causes a torque on the vehicle in the opposite direction of the propeller and the purpose of the guiding vanes is to neutralize the rotation of the vehicle by creating a torque, which is counteracting the torque from the propeller. The main purpose of the guiding vanes is to make the vehicle balanced in yaw-direction (horizontal rotation) and thereby the rudders may be used to keep the vehicle in an upright position instead of having to work with rotation.

Control System

The on-board control system is based on the DST Control developed MCU-board and a detailed description of control laws and control properties can be found in

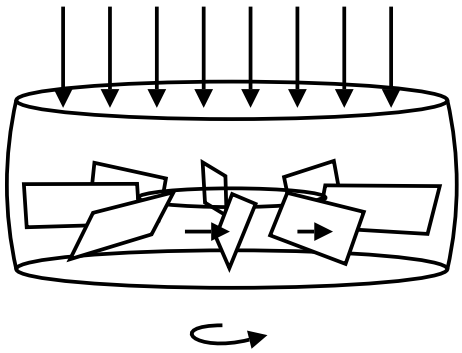

Figure 1.2. Guiding vanes.

the master's thesis [8].

1.3 Problem

The initial version of Bombus is thought to be tethered to the ground with wires. The purpose of this is to circumvent some of the regulations for flying vehicles (regulations are very restrictive regarding unmanned vehicles, however if connected to the ground the vehicle may not be considered as a flying vehicle). The tethering also acts as a safety precaution in case of a system failure during initial tests. The engine driving the propeller will also be supplied with electricity from the ground via the tethering wires.

The vehicle is intended to have an onboard control system providing for stability in the horizontal plane (roll and pitch) and the tethering device may initially control the altitude.

What kind of sensors that will be placed on the vehicle is not yet decided, however it is likely that it will have accelerometers and/or gyros. In order to use these with good accuracy it is necessary to compensate for drift in gyros and error build-up in accelerometers. The gyros have an inaccuracy (drift) caused by for example friction. These effects cannot be neglected, especially not in this case when the gyros are very small (in order to minimize weight and space). Also accelerometers give errors, however these errors are not likely to increase over time. Unfortunately, since it is necessary to integrate the acceleration twice in order to obtain the position of the vehicle, small errors in measurement of acceleration will after integration result in an error in position, which will increase over time.

Calculating a position only by estimating previous movement is in terms of navigation called "dead reckoning" or inertial navigation. However, no matter how good sensors are used and how accurate calculations are made, sooner or later the error in position will be too big. So even though the world is known (by for example a detailed map) the information will be useless since the accurate position is unknown. An external reference system is needed.

1.4 Goal

The goal of this master's thesis project is to find the most optimal technology for position and heading estimation of the vehicle. A position accuracy of 2 cm in x-, y- and z-directions and an angular accuracy of 2° in heading is the goal. The position of the vehicle is assumed to be limited to an inverted cone with diameter 10 m and a height of 25 m. The solution is supposed to work reliably under harsh outdoor conditions but also in an indoor environment. Key parameters during design are cost, reliability, robustness, accuracy and availability. A position and heading update rate of 10-20 Hz is desirable.

1.5 Related Research

In spring 2005 a university project course in control theory [6] was carried out at DST Control and has given some initial test results and a first version of a mathematical model of the Bombus vehicle. In autumn 2005 – spring 2006 a master's thesis [8] concerning modelling, control and flying capabilities of the vehicle has been done at DST Control.

1.6 Disposition

Several different technologies have been considered when trying to achieve the goal stated in Section 1.4.

In Chapter 2 an overview of all considered technologies is presented together with a brief discussion of each of them. In the following chapters the different techniques will be explained in detail together with an estimate of advantages and disadvantages of the techniques. The considered technologies are: Chapter 3: Miniature ILS, Chapter 4: Position Sensing Detector (PSD), Chapter 5: Indoor GPS, Chapter 6: Trilateration with ultra sound and Chapter 7: Global Positioning System (GPS). The techniques trilateration and PSD has been investigated in more detail than the other techniques because of being more suitable concerning cost, performance, available time and knowledge.

The PSD system was chosen as the most suitable technology and an evaluation system has been designed and implemented to evaluate the performance of this technique. The evaluation system is presented in Chapter 8 and in Chapter 9 conclusions from the evaluation system, as well as from the other investigated techniques, are described together with suggestions for improvements and future work.

Chapter 2

Candidate Solutions

Many different techniques have been considered when trying to achieve the goal stated in Section 1.4. In this chapter a brief outline of the different technologies will be given. In the following chapters the advantages and disadvantages with all the different techniques will be discussed in detail.

2.1 Solution 1: Miniature ILS

ILS (Instrument Landing System) is a widely used system at airports all over the world. The system is used primarily during bad weather conditions to guide landing aircrafts to the runway. The main principle behind the system is as follows: Two differently modulated signals are transmitted on the same frequency, one on each side of the runway. A receiver in the aeroplane separates the two signals and by comparing the signal strengths a deviation to either left or right can be detected. When the two signals have the same signal strength the aeroplane is in the correct position. Using this method in both vertical and lateral direction a "corridor" (the so called glide path) leading to the runway is obtained.

The intended solution is to modify the ILS to transmit a completely vertical glide path over the desired position and in this way a deviation in any direction can be detected. However, the ILS is designed to work with ranges of several kilometres and the main problem is likely to be whether or not the system can be adapted to such a small scale as needed in this application.

2.2 Solution 2: Position Sensing Detector

A PSD (Position Sensing Detector) is a device that has a photosensitive surface and on wich the position of a light spot on the surface can be detected. Two analogue voltages give the position in two dimensions.

In order to facilitate this solution the vehicle is fitted with four (or at least two) Light Emitting Diodes (LEDs) or laser-diodes at a suitable frequency. Through a system of lenses not very different from a normal camera the PSD is "watching the

sky" (the PSD replaces the film in the camera). If this solution is going to work it is necessary to remove all light except that from the light sources at a specific wavelength. This is done by adding an optical bandpass filter to the system, only letting the desired wavelength through. However, there is still sunlight (ambient light) on the same wavelength as the LEDs that needs to be compensated for. By modulating the LEDs with a certain frequency the constant sunlight can be filtered out as the DC-component in the output from the PSD. If the LEDs are activated one by one in a certain order the orientation of the vehicle can be estimated. The maximum operational distance of this system still remains to be investigated, but it is probable that it will be affected primarily by the intensity of the LEDs and how well the disturbing sunlight can be filtered out. According to a manufacturer of PSDs, SiTek AB [25], this can be (and has been) done with good results in similar applications, for example the following:

A position sensing system with PSD has been used in the measurement of a golf swing. A golf club was fitted with LEDs flashing in a specific order and at a known frequency. The swing was recorded with a camera fitted with a PSD instead of film. The position of the club could be plotted in two dimensions with the help of a computer. See [25] for further details.

2.3 Solution 3: Indoor GPS

Indoor GPS is a complete system provided by Arc Second [1] and is an optical, laser based, positioning system. The system is based on three (or more) fix transmitters on known locations. A receiver picks up signals from the transmitters and calculates the angles relative to the horizontal plane and a defined vertical plane. Using trigonometric formulas the position can be estimated in three dimensions with good accuracy (within the order of a few millimetres). The system can (despite its name) also be used outdoor with acceptable performance. This system requires however (at least) three fixed positions measured with good accuracy. Also the system is not designed for measuring positions at a high altitude (compared to the transmitter stations) with angles close to the vertical and the system performance for a situation like this is not known.

2.4 Solution 4: Trilateration

This method uses triangulation in three dimensions (trilateration) with ultrasound. Two ultra sonic transmitters are mounted on the vehicle on the opposite side of each other. The transmitters are preferably constructed to transmit in a wide cone directed towards the ground. Three receivers are placed on the ground (also here, as well in indoor GPS, their exact location needs to be known). In order to measure the position a starting signal is transmitted from the vehicle, either via a cable or through a radio signal (an ultrasound signal would be too slow and reach detectors at the same time as the measurement signal). At the same time as the start signal an ultra sonic pulse (measurement signal) is sent. When the receivers pick up the starting signal a clock starts counting until the measurement signal is received and

in this way the time of flight of the sound waves are measured. Using the time of flight measurements, the distances can be calculated. The calculation likely needs to compensate for air temperature in order to get a good value. Preferably is to measure the temperature both at the vehicle and on the ground. When the distances are calculated a sphere is drawn around each receiver and the position of the vehicle will (theoretically) be in the intersection of the spheres. By repeating this procedure for the two transmitters both the position and orientation in five degrees of freedom can be estimated (the rotation around the axis between the two transmitters can not be estimated).

The drawbacks with this method is the temperature dependance, which may be hard to accurately compensate for. Also the relatively large time of flight of the ultrasound signals will cause a delay in position measurement.

2.5 Solution 5: Global Positioning System (GPS)

The GPS is a worldwide, satellite based positioning system operated by the U.S. Government. The system is based on satellites in orbits around the Earth. The receiver measures the time of flight for a radio signal from one of the satellites, and in this way the distance can be calculated. By measuring the distance to three different satellites the position in three dimensions can be determined. A fourth satellite is used to set the clock in the receiver. Since the the radio signals travel with the speed of light a very accurate clock is necessary in order to measure the time of flight correctly.

A standard GPS receiver give an accuracy in the order of a few metres and an update rate of about 1 position every second, but using different enhancements an accuracy in the order of centimetres can be obtained. The major drawbacks with GPS is that it is not generally available indoors and that a receiver with high accuracy likely requires extra equipment such as accurate antennas which adds extra weight to the vehicle.

Chapter 3

Miniature ILS

The ILS system is briefly described in Section 2.1. In this chapter a more detailed description of the system together with a discussion of a possible small scale version is given.

3.1 System Overview

The ILS system consists mainly of three parts: lateral guidance, vertical guidance and marker beacons.

Lateral Guidance

A transmitter located at the end of the runway transmits two differently modulated signals on the same frequency (marked 1 and 2 in Figure 3.1). A receiver in the airplane separates the two signals, and by comparing the signal strength a deviation to left or right can be detected. When the two frequencies have the same signal strength the airplane is in the correct position (within the overlap of the two signals), the so-called glide path.

Vertical Guidance

The principle for vertical guidance is very similar to that of the lateral guidance. Two directed transmitters transmit two cone-shaped beacons, one above and one below the desired glide path (see Figure 3.2). The signals are modulated with two different frequencies and also here the position is estimated by comparing the signal levels. With the lateral and vertical guidance there is now a "corridor" leading to the runway, what is not known is the remaining distance to the runway.

Marker Beacons

The marker beacons consist of radio beacons directed straight upwards with the shape of an inverted elliptical cone. The purpose of this is to detect the remaining distance to the runway. When passing a beacon with a certain modulation

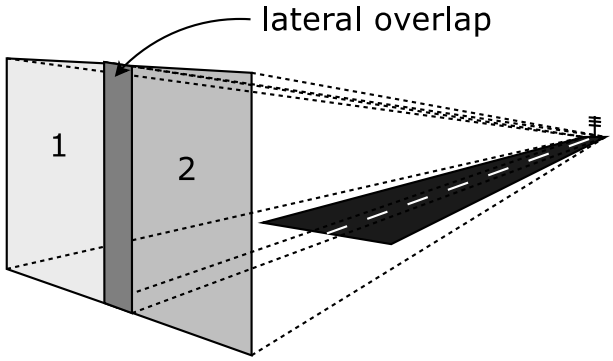

Figure 3.1. Principle of lateral guidance in ILS.

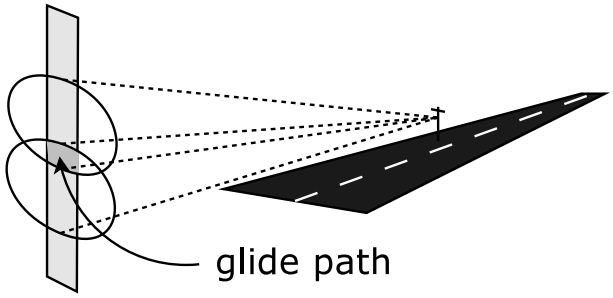

Figure 3.2. Principle of vertical guidance in ILS.

frequency the remaining distance is known. The location of the marker beacons varies within certain ranges from airport to airport. The exact location is marked on maps and can be found in navigation handbooks. The beacons are designated OM for Outer Marker, MM for Middle Marker and BM for Back Marker and can be seen in Figure 3.3.

Intended Solution

Park Air Systems [20] is the name of a company that supplies ILS systems. What has been said is that during an educational course a miniature-sized ILS system is being built in order to demonstrate the main principles. Can this system be used for position estimation? In this application a two-dimensional position in the horizontal plane may be enough, so the idea is to modify the lateral and vertical guidance to work completely vertical. By transmitting the signals straight up a "glide path" that is vertical over the intended position would be obtained and any deviations from this position could be detected. See Figure 3.4.

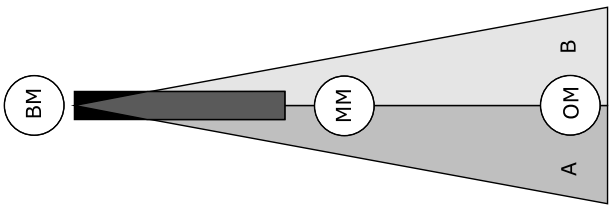

Figure 3.3. Principle of marker beacons in ILS.

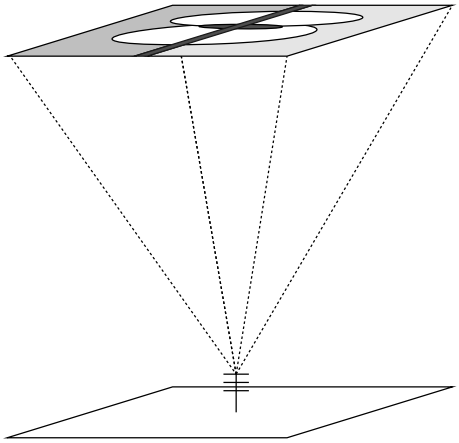

Figure 3.4. Modified miniature ILS.

3.2 System Parameters

A normal ILS system works with ranges of several kilometres, however in this application this long range is neither necessary nor desirable. A small scale version of the ILS modified to work at short ranges and being able to position the UAV within distances of up to 25 m and also fulfill the accuracy specified in the project goals is wanted. To design a system like this a number of questions arise: What frequency is suitable? What is the maximum position resolution at that frequency? Which disturbances are likely to affect the system? How robust will it be and how will it be affected by different weather conditions?

The ILS system uses different frequencies in the interval of 75-300 MHz and modulation frequencies of 90 Hz and 150 Hz. It is likely that the used frequency will affect the position resolution considerably.

Position Resolution

The position resolution is affected by the size of the overlap area (where the two signals have equal intensity). If this overlap could be made very small, the position

accuracy would be improved. However, the small scale of the miniature system makes it difficult (or even impossible) to minimize the overlap area. An antenna with very precise directional and intensity control is needed. According to Park Air Systems [20] it is likely that for this miniature system a frequency in the microwave band is necessary.

Disturbances

The miniature ILS system would be a very robust solution, free from many disturbances affecting the other methods. The interference from different weather conditions is likely to be minor, however the sensitivity for disturbances varies with the used frequency. Concern also needs to be taken to the electric field generated by the electric engine of the vehicle.

3.3 Conclusion

Since the supposed miniature system could not be used as intended, and the possibilities of constructing a miniature system as a part of this master's thesis project were limited due to time and knowledge, this method has not been investigated further. However, it is still an interesting method to investigate the future.

Chapter 4

PSD

This chapter describes the PSD system. At first an overall description of the PSD system is given, after that the different components and subsystems are described. In Section 4.2 the basic principles behind the PSD and also different kinds of PSDs are described. In Section 4.3 some optical principles affecting lenses and imaging systems are discussed. In Section 4.4 different kinds of light sources and modulation techniques are described and finally in Section 4.5 the interpretation of the measured result is described. The implementation of the PSD system is described in Chapter 8.

4.1 System Overview

In Figure 4.1 a schematic overview of the measurement system is shown.

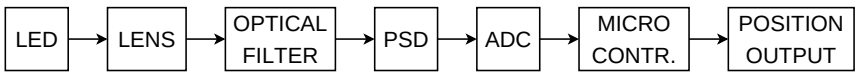

Figure 4.1. Overview of the PSD system.

The Light Emitting Diode (LED) emits radiation (light) at a specific wavelength. The light sources may be modulated to increase the filtering options. The lens collects all light and after passing through an optical filter the light is projected on to the PSD. The output from the PSD is read by an Analogue to Digital Converter (ADC) and the digital result is an input to the microcontroller. The microcontroller calculates the position, which is then transmitted as an output and may be used for control purposes of the UAV.

4.2 PSD - Position Sensing Detector

In this section the functional principle of the Position Sensing Detector (PSD) will be presented. The information mainly comes from [27], [26], [21] and [23]. In short a PSD is a device that from an incident light spot gives an output, which is proportional to the position of the light spot.

History

The key element in the positioning system is of course the Position Sensing Detector (PSD). The PSD was invented at around 1971 by L E Lindholm and G Petterson, two engineers at Chalmers University of Technology, Göteborg, Sweden [26].

4.2.1 Semiconductors

The information on semiconductors used in this section is given mainly in [27]. A semiconductor is often created by taking for example silicon and adding an impurity in the material. The atoms in silicon are ordered in a crystalline pattern, which can be seen in Figure 4.2. When an impurity is added some of the atoms in the lattice are replaced.

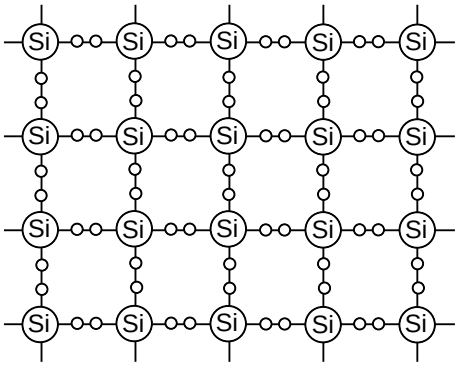

Figure 4.2. The molecular structure of silicon.

What element to add depends on what properties the final semiconductor should have. If adding for instance arsenic (As) the situation in Figure 4.3 is obtained.

The arsenic atoms have five valence electrons, compared to silicon which has four. When put together like this, there is "no room" for the fifth electron of the arsenic atom, which will be loosely bound and easily excited. If the fifth electron is excited (by for example light or heat) it will move to the conduction band of the atom, thus making it possible for charges to move over the surface of the semiconductor. This is a conductor of which the conducting properties can be controlled, i.e. a *semiconductor*.

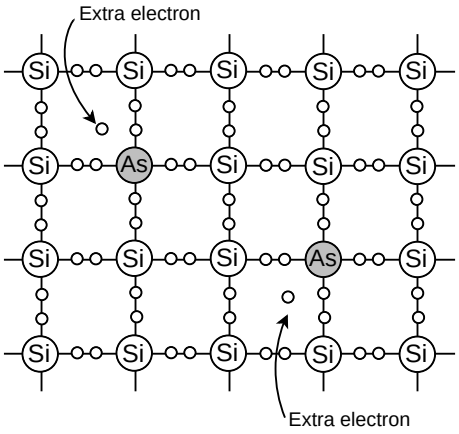

Figure 4.3. *n*-doped semiconductor.

If an element with extra electrons is added to silicon a *n*-type semiconductor is obtained. It is called *n*-type because the charge carriers are negative electrons.

In a similar way an element with for example three valence electrons can be added, but in this case there will be a lack of electrons, positive "holes" in the valence band. The holes are in reality "lack of electrons", thus creating a less negative (i.e. "positive") area. These holes can move between atoms if for example an electrical field is applied. This is called a *p*-doped semiconductor since the charge carriers are positive holes.

pn-junction

A *pn*-junction consists of two differently doped materials attached to each other. The *n*-doped material contains loosely bound electrons and a *p*-doped material contains "holes". This is shown in Figure 4.4.

At the border between the two materials diffusion will take place. Electrons will diffuse from the *n*-side over to the *p*-side where the concentration of electrons are a lot lower. In a similar fashion the holes will diffuse from the *p*-side to the *n*-side. The holes and electrons will however not move very far since the semiconductor is not a very good conductor. Because of this the excess of negative electrons on the *p*-side and the positive holes on the *n*-side respectively, will create a double layer of positive and negative charges at the junction of the *p*- and *n*-side. This is shown in Figure 4.4. This layers of charge will in turn create a potential difference over the junction, with the *n*-side at a higher potential than the *p*-side. The conducting properties of the *pn*-junction can be controlled by applying a voltage over it, thus creating a diode. This principle is the foundation for all semiconductors.

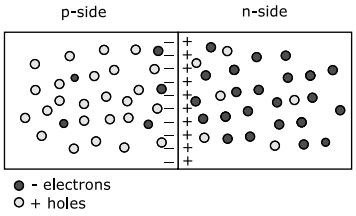

Figure 4.4. *pn*-junction.

Forward and reverse bias

If the *pn*-junction is connected to a voltage supply and a resistor, a simple diode is created. The *pn*-junction diode can be operated in two different modes: the forward bias mode and the reverse bias mode.

In forward bias mode, the *p*-side is connected to the positive terminal of the voltage supply as shown in Figure 4.5. The applied voltage has the effect of lowering the potential difference over the junction, thus making it easier for electrons to diffuse from one side to the other resulting in an electrical current flowing through the circuit.

In reverse bias mode the situation is the opposite: The *p*-side is connected to the negative terminal of the voltage supply. This will increase the potential across the junction, making it difficult for the electrons to diffuse and no current will flow through the circuit. The diode is acting as an insulator as long as no external energy is added. See Figure 4.6

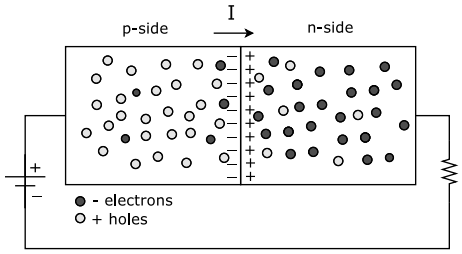

Figure 4.5. *pn*-junction in forward bias mode.

Photodiodes and Solar Cells

A photodiode uses light to enhance the diffusion of electrons over a *pn*-junction: The *p*-side is exposed to sunlight and photons may excite one of the electrons in an atom, making it very loosely bound. The electron can then leave its orbital in the atom and then leaving a hole; an electron-hole pair is created. The *p*-side is already rich with holes and some electrons will just recombine with the first

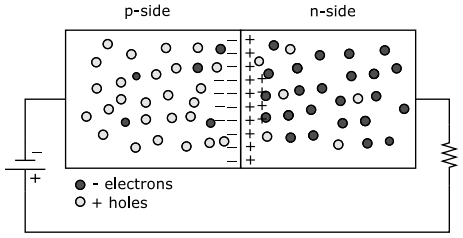

Figure 4.6. *pn*-junction in reverse bias mode.

hole that comes in their way, but some of them will migrate to the junction. Due to the electric field caused by the different charges in the junction, the electrons will accelerate into the *n*-side. This creates an excess of negative charge at the *n*-side and an excess of positive charge at the *p*-side. The result is a difference in potential and if the two regions are connected through a resistor the charges will flow from one side to the other. See Figure 4.7.

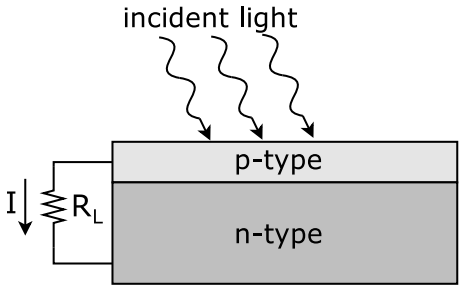

Figure 4.7. The functional principle of a solar cell.

Thus the incident light has been converted to electrical energy, i.e. a solar cell is created. The current in the resistor is proportional to the number of photons hitting the surface, which in turn is proportional to the intensity of the incident light [27].

The photodiode can be operated in two different modes: the photovoltaic mode and the photoconductive mode. The photovoltaic mode corresponds to the forward bias mode and the photoconductive mode is similar to the reverse bias mode.

The PSD

The PSD is basically a large photodiode. The information about PSDs is taken from [21], and a schematic view of the PSD is shown in Figure 4.8. The PSD is normally operated in the photoconductive mode, that is, the *pn*-junction is reverse biased. A positive potential is applied to the *n*-layer in the bottom of the PSD. On the *p*-layer two metal electrodes are placed, one on each side. Since the *pn*-

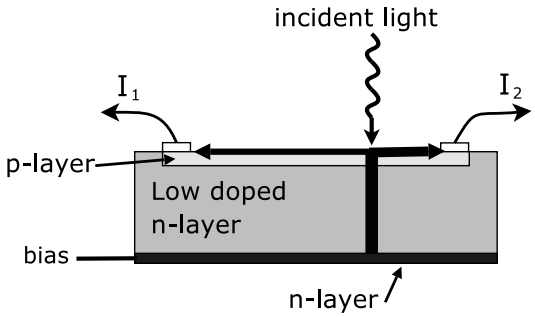

Figure 4.8. Schematic view of a PSD.

junction is reverse-biased no current will flow when there is no incident light on the surface (except for a small leakage current, the so-called dark current). When incident light is present, electrons will break loose from the atoms and a current will flow from the *n*-layer to the *p*-layer and then be divided between the two electrodes.

However this is still only a photo detector, but if the *p*-layer is made to have a homogenous resistance, the current output from one of the electrodes can be written

$$I = \frac{U}{R(L)} \tag{4.1}$$

The current I depends inversely on the distance travelled, L, from the light spot to the electrode in the resistive layer. By comparing the output from the two electrodes the relative position of the incident light can be calculated. The intensity of the light of course affects the size of the two currents, but if compared with each other the intensity dependence cancels out. This is the principle of a one dimensional position sensing detector (1D-PSD). To create a two dimensional detector the same principle is used but in two orthogonal directions. Two different versions exist, the duo-lateral and the tetra-lateral PSD.

4.2.2 Duo-lateral PSD

The difference between duo-lateral and tetra-lateral is mainly the number of outputs from the same layer [21]. In the duo-lateral version electrodes are placed both on the upper *p*-layer and on the bottom *n*-layer (see Figure 4.9).

If both the *n*-layer and the *p*-layer are processed to be resistive, one position coordinate, X, can be extracted from the upper side and the other position coordinate, Y, from the bottom side. The advantages of having the electrodes on different sides of the detector are that they do not affect each other.

The 2D tetra-lateral type has all four electrodes on the upper side, which causes decreased linearity in the corners where the electrodes are close to each other. An advantage is that the output current is twice as high for the duo-lateral PSD

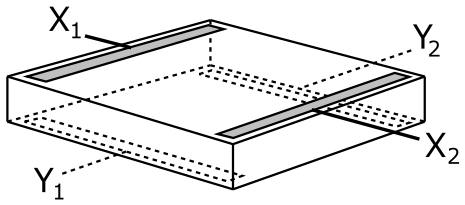

Figure 4.9. Principle of a 2D duo-lateral PSD.

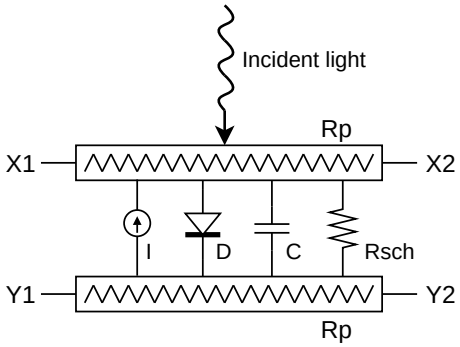

Figure 4.10. Equivalent electric circuit of 2D duo-lateral PSD.

compared to the tetra-lateral PSD, this because the current is divided over only two electrodes instead of four. A higher current implies a better signal to noise ratio, which in turn increases position resolution.

The duo-lateral PSD is operated in the photovoltaic mode (forward bias). The equivalent electrical circuit of a duo-lateral PSD is shown in Figure 4.10 [21].

The position for a light spot on a 2D duo-lateral PSD can be calculated using

$$X = \frac{I_{X2} - I_{X1}}{I_{X1} + I_{X2}} \cdot \frac{L_X}{2} \tag{4.2}$$

$$Y = \frac{I_{Y2} - I_{Y1}}{I_{Y1} + I_{Y2}} \cdot \frac{L_Y}{2} \tag{4.3}$$

where the origin of the coordinate system is located at the centre of the PSD and L_X and L_Y is the length of the active area in x- and y-directions respectively.

4.2.3 Tetra-lateral PSD

The 2D tetra-lateral PSD has the structure shown in Figure 4.11 [21]. In this case all the four electrodes are placed on the same resistive upper surface. The photocurrent generated from incident light is divided over the four electrodes placed

along the edges. Interaction between the electrodes in the corners of the active surface causes position distortion and decreased linearity for this type of PSD. However, the tetra-lateral PSD can easily be reverse biased by applying a voltage to the common electrode and hence decreasing dark current and enhancing response speed. The equivalent electrical schematic of the 2D tetra-lateral PSD is shown in Figure 4.12. The position is calculated from the output currents in the same way as for the duo-lateral type, described in (4.2) and (4.3).

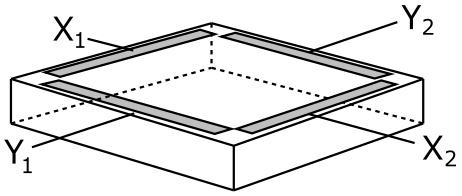

Figure 4.11. Principle of a 2D tetra-lateral PSD.

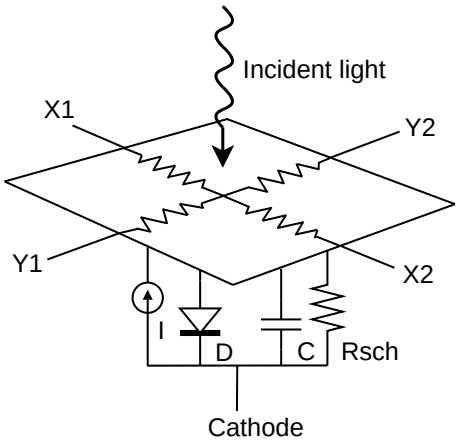

Figure 4.12. Equivalent electric circuit of 2D tetra-lateral PSD.

4.2.4 Improved Tetra-lateral PSD

This is a variant of the tetra-lateral type PSD with improved active area and reduced interaction between electrodes, giving it the advantages of the tetra-lateral PSD but without the decreased linearity in the corners. This type is also called pin-cushion type. A schematic picture of the pin-cushion type and the corresponding electrical equivalent is shown in Figures 4.13 and 4.14 respectively.

The position calculation for the improved tetra-lateral type PSD is somewhat different from the duo-lateral and tetra-lateral PSD. The position can be calculated

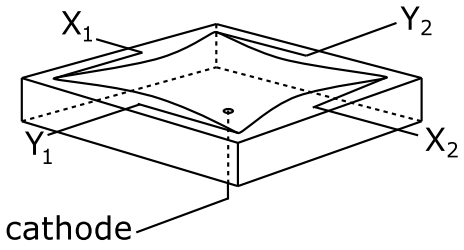

Figure 4.13. Principle of an improved tetra-lateral (pin-cushion) PSD.

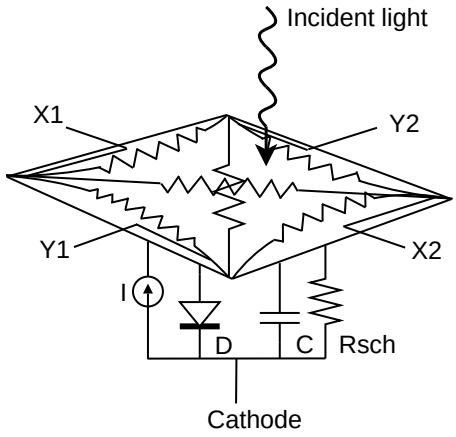

Figure 4.14. Equivalent electric circuit of an improved tetra-lateral (pin-cushion) PSD.

as

$$X = \frac{(I_{X2} + I_{Y1}) - (I_{X1} + I_{Y2})}{I_{X1} + I_{X2} + I_{Y1} + I_{Y2}} \cdot \frac{L_X}{2} \tag{4.4}$$

$$Y = \frac{(I_{X2} + I_{Y2}) - (I_{X1} + I_{Y1})}{I_{X1} + I_{X2} + I_{Y1} + I_{Y2}} \cdot \frac{L_Y}{2} \tag{4.5}$$

Also here the centre of the coordinate system is located at the centre of the PSD and L_X, L_Y is the length of the active area of the PSD in x- and y-directions respectively.

4.2.5 Dark Current

If the PSD is reverse biased and placed in darkness a small current will flow through the circuit. This current is called dark current or leakage current. The dark current depends on temperature and also the size of the PSD.

Position Resolution

The PSD detector has a resolution better than $1\,\mu$m, i.e. $10^{-6}\,$m under optimal conditions [21].

4.3 Optics

In this section the optical design parameters of the measurement system will be discussed. Information is taken from [11] and [24].

4.3.1 Basic Optics

Lenses and Imaging

The lens is the main component in an optical system. The image of an object projected through a lens can be calculated using the lens formula

$$\frac{1}{f} = \frac{1}{a_1} + \frac{1}{a_2} \tag{4.6}$$

In Figure 4.15 a basic lens system is shown.

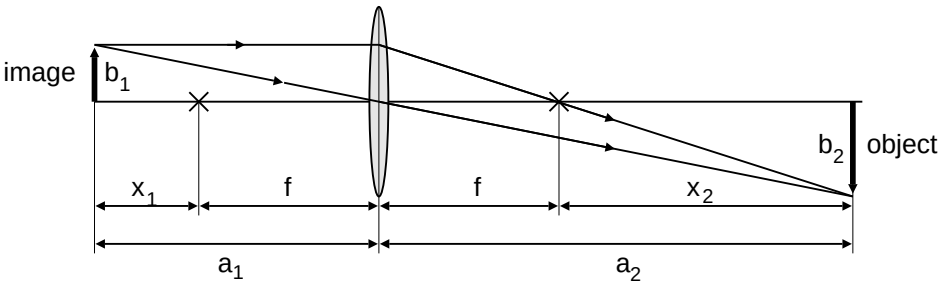

Figure 4.15. A simple lens system.

Magnification is defined as

$$M = \frac{b_1}{b_2} \tag{4.7}$$

4.3.2 Imaging Systems

Aperture and Shutter

The aperture is a device mounted in objectives and system of lenses in order to limit the amount of light into the system. In a photographic camera there is also a shutter that opens when the picture is taken. The amount of light hitting the film is controlled by the size of the aperture and how long time the shutter is open.

The size of the aperture is also affecting the depth of field (described later in this section).

Field of View

Field of view (FOV) is defined as the maximum angle that can be seen with a certain objective. FOV can be calculated in a rather simple way using the lens formula (4.6) together with some geometric and trigonometric formulas and Figure 4.16. This gives

$$\frac{h}{a_1} = \frac{h'}{a_2} \tag{4.8}$$

$$\alpha = arctan\left(\frac{h'}{a_2}\right) \tag{4.9}$$

$$FOV = 2 \cdot arctan\left(\frac{h'}{a_2}\right) \tag{4.10}$$

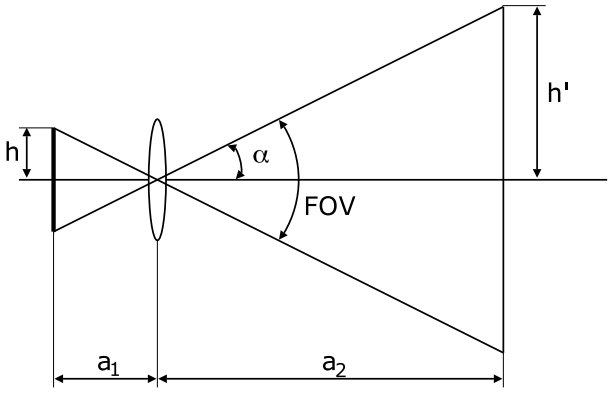

Figure 4.16. Field of view (FOV) of an optical system.

Since the lens is circular, the visible area will always be circular and projected as a circle on the image plane. In cases when a square or rectangular picture is wanted, the detector area is simply an area inside of the circle and the light outside the detector is ignored. This means that if the detector is rectangular, a different FOV will be obtained in the horizontal and the vertical directions respectively.

Depth of Field and Depth of Focus

In an imaging system such as a photographic camera only an object at a certain distance can give a sharp image, everything else in the picture will be more or less blurred. This can be seen by studying the lens formula (see (4.6)): For a given lens with focal distance f and an object at a fixed distance a_1 only one value is possible for a_2, i.e. *only* at distance a_2 will the object be in focus and sharp. But

what is sharp? Sharpness is of course limited by the "detector" that is watching the image, for example the human eye or a PSD. The resolution of a detector can be defined in several ways, a common definition is the following: "Resolution is the smallest distance between two objects in an image that makes it possible to still separate them from each other" [24].

Most often something that is to be imaged has an extension in three dimensions and does not have an exact distance from the lens to the object but instead varies within a certain interval. In order to be able to handle this a *blur circle* or *circle of confusion* is defined as the maximum allowed blur that is still considered sharp. For the human eye for example, at a distance of 25 cm and during good conditions a line of width 0.075 mm can be perceived. This distance is equivalent to a distance of about 5 μm at the retina in the eye. The performance is limited by the granular structure of the retina, consisting of light receptors of finite size.

The Depth Of Field (DOF) is thus defined as *the interval within which, all objects give an image with a blur less than the circle of confusion.*

The following definitions are explained in detail in [24], and also the same designations have been used. S and R is the far and near limits of the depths of field respectively and calculated according to (4.11) and (4.12). The total DOF, T, is given in (4.13). These equations are valid when the object distance $u \gg v$.

$$S = \frac{uf^2}{f^2 - NCu} \tag{4.11}$$

$$R = \frac{uf^2}{f^2 + NCu} \tag{4.12}$$

The total DOF is given by

$$T = S - R = \frac{2f^2u^2NC}{f^4 - N^2C^2u^2} \tag{4.13}$$

where u is the distance to the object, f the focal distance, N the aperture and C the circle of confusion. In Figure 4.17 the DOF is illustrated.

The depth of field is thus dependent on the allowed blur in the image, the circle of confusion. Once the allowed circle of confusion *in the image* is determined, the depth of field can be determined using the formulas above. The depth of field is thus an interval where all objects within the interval are imaged with a blur less than or equal to the circle of confusion.

It is common to distinguish between *depth of field* and *depth of focus*. The first is used when referring to real distances, for example between two objects that are to be photographed and the latter is used when dealing with the *image*, depth of focus is a distance in the image plane. In this master's thesis the abbrevation DOF refers to *Depth of Field*.

In the case of the PSD positioning system a DOF of about 0–25 m would be optimal.

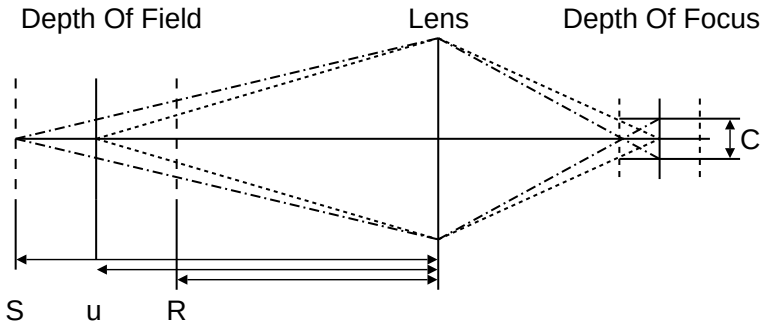

(a) Far Depth Of Field.

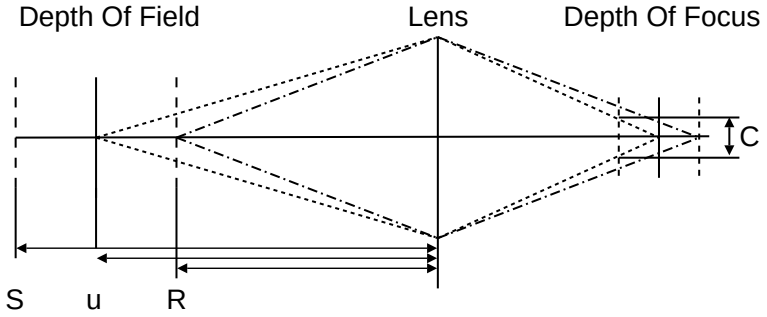

(b) Near Depth Of Field.

Figure 4.17. Depth of Field, DOF, and Depth of Focus.

Hyperfocal Distance

The hyperfocal distance, h, is defined as the value of a particular focus setting, u, which makes the far depth of field,S, tending to infinity. By studying (4.11) it is seen that if $f^2 = NCu$ the denominator equals zero and S goes towards infinity. By adjusting focus to the hyperfocal distance the DOF will be from $\frac{h}{2}$ to infinity and it yields

$$S = \frac{hu}{h-u} \tag{4.14}$$

$$R = \frac{hu}{h+u} \tag{4.15}$$

The total DOF is given by

$$T = \frac{2hu^2}{h^2-u^2} \tag{4.16}$$

The hyperfocal distance is often used as focus setting in simple so called “focus free” cameras, because the user does not have to care of more than being beyond the near limit of the DOF.

4.3.3 Optical Aberrations

The lens formula and other formulas used in optics often assume perfect lenses, but in reality however a number of optical aberrations affect the lenses. For example coma, astigmatism, curvature of field and distortion are optical defects that occur in a system of lenses such as an objective. Most lenses are adapted for the visible spectrum, so if other wavelengths are to be used (such as IR or UV) there may be a need to use IR/UV-corrected lenses. The reason for this is that light of different wavelengths refracts differently in a lens (refraction index depends on wavelength [11]), and thus for example red and blue light will be focused at different points on the optical axis. This is called chromatic aberration and there are different techniques to reduce or cancel out this effect, for example by using a so called chromatic doublet which consist of a pair of lenses that when combined have the same focal distance for two colours [11]. These defects are treated in detail in [24] and no further concern will be given here. In the evaluation system built (described in chapter 8) the optical defects are assumed negligible compared to other inaccuracies in the system.

4.3.4 Sunlight

The sun emits enormous amounts of electromagnetic radiation. The sun can be approximated with an ideal blackbody at temperature 5800 K [16, 27]. In Figure 4.18 radiation spectrum for an ideal blackbody at temperature 5800 K is shown. The visible wavelengths between 400–700 nm are marked in the figure. A great deal of radiation is absorbed in the atmosphere though, and how much that reaches the earth surface vary a lot between different locations and different seasons.

4.3.5 Wavelength

For a PSD measurement system a light source with wavelength somewhere outside the highest intensity of the sun radiation is desirable, for example in the IR band (above 700 nm) or UV band (below 400 nm). Another consideration that has to be made is that a standard PSD sensor has a spectral response between about 400–1100 nm, with maximum response for 950 nm [21]. There are also special UV-enhanced PSDs also sensitive to UV radiation with a spectral response between about 200–1100 nm. However, also for the UV type of PSD the maximum spectral response is at 950 nm. The spectral response of a standard PSD is shown in Figure 8.3(b) in Section 8.2.

4.3.6 Filters

Optical filters are needed in order to reduce the amount of light that reaches the PSD sensor. There are two main types of filters: interference filters and coloured glass. Coloured glass filters tend to be less expensive, but can not be made as “narrow” as an interference filter. An interference band pass filter can be made to only transmit wavelengths within a few nanometres.

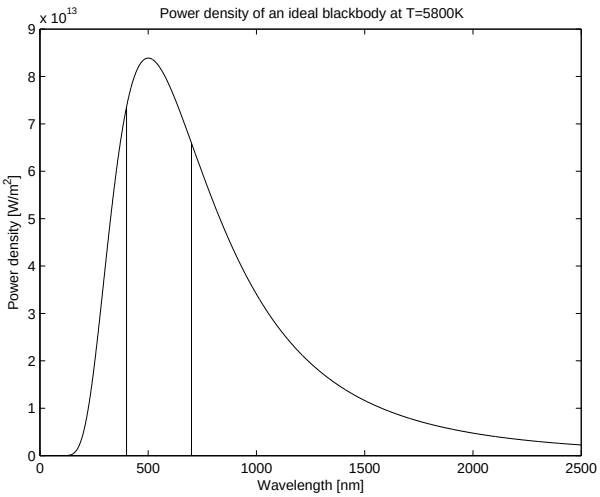

Figure 4.18. Radiation of an ideal blackbody at temperature 5800K. The visible wavelengths between 400 – 700 nm are marked.

Coloured Glass

A coloured glass filter is simply a piece of coloured glass, which absorbs certain wavelengths and transmits others. For example a red filter transmits wavelengths in the red area and absorbs all other wavelengths. This is also the reason that it looks red: When hit by white light (all colours) "everything" is absorbed except the wavelengths in the red spectrum which are partly reflected and seen by the eye.

Interference Filters

Interference filters use the wave properties of light to create destructive interference and often also incorporate a coloured glass filter. Interference filters are very sensitive to the direction of incident light and light almost perpendicular to the filter surface is necessary for the filter to work well.

4.4 Light Source

The light sources are thought to be mounted on the vehicle. To be able to determine the heading of the vehicle it is either necessary to know which light source is turned on at a specific time or by giving each light source a specific ID-sequence which makes it possible to distinguish them from each other.

4.4.1 Modulation

In order to reduce disturbances from surrounding light modulation can be used. A simple amplitude modulation is On Off Keying (OOK) which works in the following way [19]: A carrier frequency f_0 is multiplied by "0" or "1". A signal with the specified frequency equals a logical "1" and zero signal equals logical "0". In Figure 4.19 the principle of OOK is illustrated. This is the same principle used in ordinary remote controls used in for instance TV-sets and DVD players among other things.

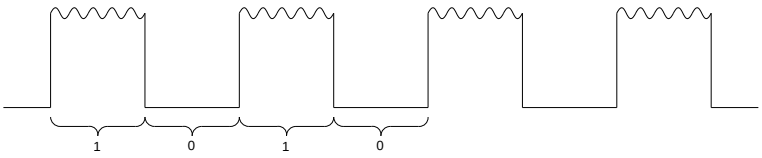

Figure 4.19. On Off Keying (OOK) modulation.

4.4.2 Demodulation

The demodulator is more or less a bandpass filter constructed for the specified carrier frequency of the light source. When a signal with the frequency f_0 is received a logical "1" is obtained and otherwise logical "0". Sometimes the levels may be inverted for practical reasons.

4.5 Interpretation

A microcontroller is used to interpret the output from the PSD. The output signal is sampled with an Analogue to Digital Converter (ADC) and then read by the microcontroller. The microcontroller uses more or less the lens formula to calculate the position of the light source. The altitude can be estimated by comparing a distance on the vehicle with the measured distance and the orientation of the vehicle is calculated as the angle between the two light sources.

4.6 Conclusion

The PSD system combines high accuracy with a possible high update rate. The system performance is depending on the ability to filter out disturbing light though. In order to further evaluate the technique an evaluation system with PSD has been built, and in Chapter 8 further details are described.

Chapter 5

Indoor GPS

The Indoor GPS system is a complete position measurement system supplied by Arc Second [1]. In this chapter a brief introduction describing the main principles behind the system will be given. This is followed by an evaluation of the expected system performances. Information is taken from the company home page and includes white papers [12] and product information [2].

5.1 System Overview

The Indoor GPS system works on a somewhat similar principle as the Global Positioning System (GPS), described in Section 2.5. The Indoor GPS is based on transmitter stations placed at known locations. Using two transmitter stations it is possible to determine the position of a receiver in three dimensions. A standard accuracy of approximately 1 mm in x, y, z can be achieved and if more transmitter stations are added the accuracy can be increased further. There are also other methods that can be used to enhance accuracy, for example the use of reference receivers at known location. The reference receivers can be used to calibrate the system in a similar way as the differential GPS (DGPS) or WAAS is used in GPS. With the use of this enhancements, an accuracy of up to 0.1 mm may be achieved. By placing multiple receivers on the measurement object an accuracy of up to 0.050 mm can be achieved [3].

5.2 Position Calculation

The position is calculated by measuring the horizontal (azimuth) and vertical (elevation) angles to the transmitter stations. The transmitter stations transmit three signals: Two rotating infrared laser "fan beams" and one infrared LED strobe. The laser beams are transmitted as shown in Figure 5.1 and are rotating with known speed. The laser beams are tilted from the vertical plane with angle $\phi \approx 30°$. The different transmitters can be set to rotate with different speed and thereby the transmitters can be identified.

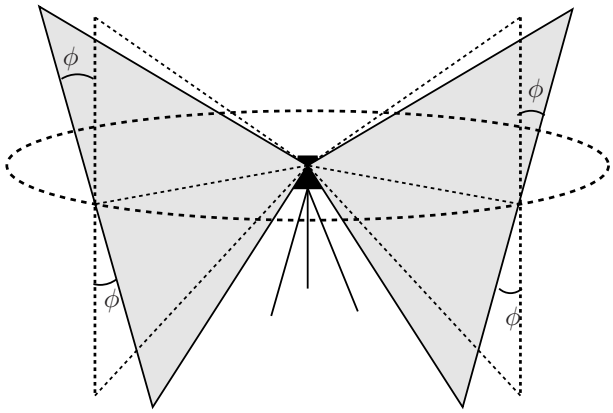

Figure 5.1. Principle of vertical angular measurement in Indoor GPS.

Elevation

The elevation (vertical angle) is measured by calculating the timing difference between the two beams shown in Figure 5.1. A long time difference indicates an angle near vertical above the horisontal plane, while a short time difference indicates an angle near vertical, *below* the horisontal plane.

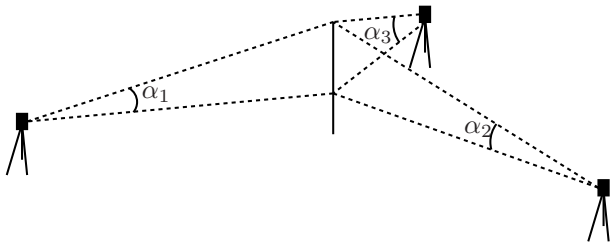

Figure 5.2. Vertical angle (elevation) measurement in Indoor GPS.

Azimuth

The azimuth (horizontal angle) is measured with use of the LED strobe signal. The LED strobe is always fired at the same point in the rotation of the transmitter. The horizontal angle is measured by making a time measurement between the strobe and the laser pulses. Since the speed of rotation is known the angle to the actual position can be calculated. If the time is measured to a point in the middle between the two pulses (as shown in Figure 5.3), the vertical angle does not have to be known to calculate the horizontal angle.

Once the azimuth and elevation have been measured the three dimensional

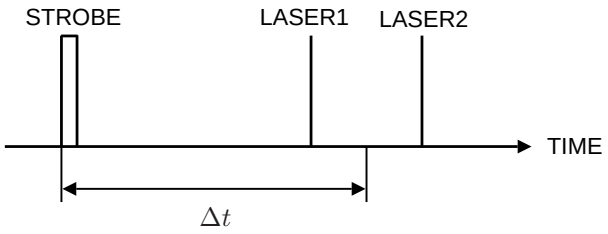

Figure 5.3. Principle of horisontal angular measurement in Indoor GPS.

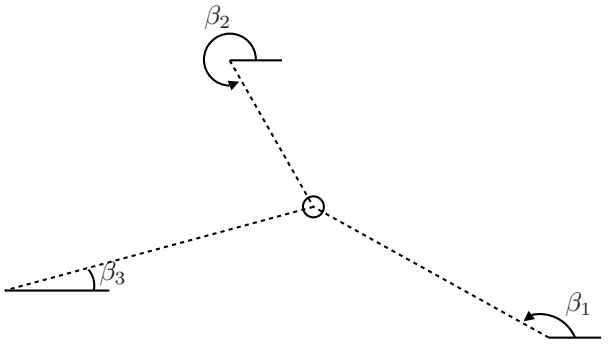

Figure 5.4. Horizontal angle (azimuth) measurement in Indoor GPS.

position can be determined. In Figure 5.2 and 5.4 the geometry of the position calculation is shown. The system has a position update rate of 55 Hz.

5.3 Accuracy and Disturbances

According to the product information [3] an accuracy of 1 mm and up to 0.05 mm is possible. To be able to achieve this high level of accuracy indoor use is however assumed. In an outdoor environment the sunlight becomes the main error at long ranges. The system has been tested outdoors in the application of guiding an autonomous lawn mower on a football field with good results [1]. No values for outdoor precision are however given in the product information though.

5.4 Conclusion

The Indoor GPS system is primarily intended as a high accuracy indoor measurement system, although it also can be used outdoor. However the system performances for an application such as investigated in this thesis is not known. When used for positioning of an aerial vehicle, the angle between the transmitter sta-

tions and the vehicle will likely be close to vertical, and the system is not designed for operation during conditions like this. The system is also probably not likely consistent with the low cost goal of the project.

Chapter 6

Trilateration

Measuring three distances to known locations and in that way calculate the position is called trilateration. The method described in this section uses trilateration with ultra sound, and a brief description of the method is given in Section 2.4. An error/performance analysis of the method will also be done, however on a theoretical basis only. The method for solving the position equations presented in this chapter is proposed in [15].

6.1 System Overview

A schematic overview of the system is shown in Figure 6.1.

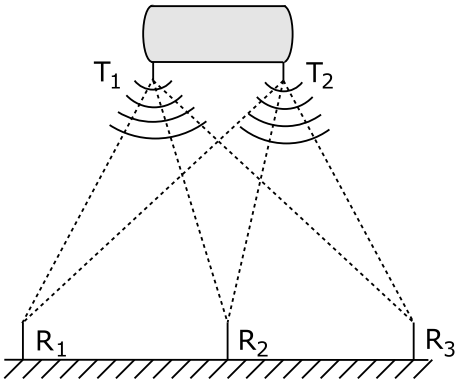

Figure 6.1. Schematic view of the system.

At least two ultrasound transmitters (T_1, T_2) are placed on the UAV. On the ground (at least) three receivers (R_1, R_2, R_3) are placed. To be able to determine the orientation of the vehicle two transmitters are needed, using only one transmitter gives the coordinates of one point but no information about the

orientation of the vehicle. To produce a three dimensional position estimate three receiver station are required.

If more than two transmitters or more than three receivers are used, an opportunity to error correction occurs since the system of equations are over determined. This kind of system is generally not solvable without the use of an approximation method, such as for example the least square method. Since more measurements are used, and therefore the effect of individual measurement errors are diminished, it may be possible to achieve a higher level of accuracy. This case will however not be treated in this master's thesis, here the case with only two transmitters and three receivers is considered.

The three dimensional position vectors of the receivers relative to a reference point are necessary. The final position measurement will be given from this reference position.

To start a measurement a starting signal is transmitted at the time t_0, and at the same time a measurement signal is sent. The starting signal needs to be considerably faster than the measurement signal for this to work, (more about this in Section 6.4). The starting signal tells the receivers to start a time measurement. The clocks in the receivers start counting until they receive the ultra sonic position measurement signal. Each receiver then has a unique time measurement which is proportional to the distance between the receiver and the transmitter on the vehicle.

A sphere can be drawn around each receiver with the radius corresponding to the measured distance. Theoretically the transmitter (and thus the vehicle) will be located in an intersection between the spheres. The coordinates of the transmitters will in this way be determined in three dimensions. Now the position (of any point on the vehicle) and the orientation can be determined using vector calculation.

6.2 Speed of Sound

The speed of sound will of course have a great impact on this method. Unfortunately the speed of sound is not constant but varies greatly with temperature. If this method is going to produce any useful results it is necessary to measure the temperature and compensate for it.

In Appendix B the following expression for the speed of sound is derived:

$$v = \sqrt{\frac{\gamma p}{\rho}} \tag{6.1}$$

depending on the pressure p, density ρ and the constant γ.

Temperature Dependance

Using the ideal gas law (6.1) can be rewritten to depend on temperature instead of pressure and density:

$$pV = nRT = \frac{m}{M}RT \Rightarrow \tag{6.2}$$

$$p = \frac{m}{V}\frac{RT}{M} = \rho\frac{RT}{M}$$

where M is the molar mass, R the universal gas constant and T the temperature in Kelvin. Combining (6.2) with (6.1) gives

$$v = \sqrt{\frac{\gamma RT}{M}} \tag{6.3}$$

Here ρ cancels out, and thus the propagation speed depends on the temperature, the (known) universal gas constant and the molar mass of air.

Molar Mass of Air

The atmosphere of the earth consist mainly (99.9%) of three gases: nitrogen(N_2), oxygen (O_2) and argon (Ar). The relative composition of the atmosphere is shown in Table 6.1.

Element	Amount (% of mass)	Molar mass [g/mole]
N_2	75.54	28.013
O_2	23.10	31.999
Ar	1.3	39.948

Table 6.1. Relative composition of the atmosphere of the earth [9].

The molar mass of air is approximately

$$M_{air} = 0.231 \cdot M_{O_2} + 0.7554 \cdot M_{N_2} + 0.013 \cdot M_{Ar} \tag{6.4}$$

$$M_{air} \approx 29.072 \approx 29\, g/mole \tag{6.5}$$

The speed of sound in air can thus be written according to (6.3) where the temperature, T, is the only unknown parameter.

6.3 Distance Calculation

When a measurement is complete, an estimate of the distance is needed in order to calculate the position. Since the temperature is not constant at different altitudes, neither will the speed of sound. the distance can be calculated using the simple and well known formula $d = v(T)t$, where d is the distance, $v(T)$ the speed of sound at temperature T and t the measured time.

Temperature

The temperature can be measured at the three receiver stations and also at the vehicle. To keep a good measurement accuracy the temperature needs to be measured as accurately as possible. Even if the temperature is measured at two positions, for example at the vehicle and at one of the measurement stations, nothing

is known about the temperature between these two points. In the following calculations the temperature is assumed to vary linearly between the two measurement points. If this is a reasonable approximation or not depends of courses on the conditions at the specific location where the vehicle is being operated. However, if a more precise temperature distribution is known it is easy to modify the calculations and otherwise this is a reasonable assumption.

Distance

In this section an expression for calculating the distance between two points, given the measured time, will be derived. The temperature distribution is assumed linear between the two known temperatures, the temperature at the vehicle, T_v, and the temperature at the i:th measurement station, T_i. The temperature distribution is a function of the travelled distance d. The temperature distribution can be written as

$$T(h) = T_i + \frac{T_v - T_i}{h_v} \cdot h \tag{6.6}$$

where h_v is the height at which T_v is measured. The expression (6.3) for the speed of sound can now be written as

$$v(T) = v(T(h)) = v(h) \tag{6.7}$$

Inserting the expression for v as in (6.3) and approximating $d \approx h$ gives

$$d = v(d)t = \sqrt{\frac{\gamma RT(d)}{M}} \cdot t \quad \Rightarrow \quad d^2 - \frac{\gamma RT(d)}{M} \cdot t^2 = 0 \tag{6.8}$$

$$d^2 - \frac{\gamma Rt^2}{M}\left(T_i + \frac{(T_v - T_i)}{h_v} \cdot d\right) = 0 \tag{6.9}$$

$$d^2 - \frac{\gamma Rt^2(T_v - T_i)}{Mh_v} \cdot d - \frac{\gamma Rt^2 T_i}{M} = 0 \tag{6.10}$$

$$ad^2 + bd + c = 0 \tag{6.11}$$

If the positive root for d is chosen (since $d \geq 0$), the distance can be calculated as

$$d = \frac{-b + \sqrt{b^2 - 4ac}}{2a} \tag{6.12}$$

where

$$a = 1 \tag{6.13}$$

$$b = -\frac{\gamma Rt^2(T_v - T_i)s}{h_v} \tag{6.14}$$

$$c = -\frac{\gamma RT_i t^2}{M} \tag{6.15}$$

The distance can now be calculated from a measured time, although one problems remains: The temperature distribution is assumed vertical but the distance

measurement is not likely to be vertical (unless the location of the vehicle is directly above one of the measurement stations). This effect can either be neglected (since the vehicle is intended to operate in a limited area above the measurement stations) or the difference between d and h can be calculated using the previous position measurement and the known positions of the measuring stations. It is also likely that the error from the assumed linear temperature distribution has a greater impact on the result than the altitude–distance approximation.

As h_v the previous altitude measurement can be used, assuming the altitude does not change very quickly.

6.4 Transmitters

The transmitters consist of an ultra sonic transmitter and a "send-start-signal device".

The reason for choosing ultrasound is that it moves relatively slow in air ($v_{sound} \approx 330\,\mathrm{m/s}$) and by that making it possible to measure the time of flight in an easy way. A clock working in a speed of about 1 MHz will give a reasonable measurement. However, the slow speed of the ultrasound is also a problem of the measurement system: there will always be a delay of the output caused by the time of flight.

The start signal can for example be a radio signal, an optical signal or a signal sent over a cable. However, it is essential that the start signal is considerably faster than the measurement signal itself. There are two reasons for this:

- If the starting signal is fast enough, the delay during its time of flight can be neglected.
- The fact that it probably takes a different amount of time to reach the different transmitters (causing them to start the measurement at different times, hence giving erroneous measurements) can in this case also be neglected.

If for example the vehicle is located at a height of 20 m and a radio signal is used as start signal (propagating with speed $v_{radio} = c =$ speed of light) the time of flight will be

$$t_{start} = s/v_{radio} = 20/3 \cdot 10^8 \approx 6.7 \cdot 10^{-8} s \tag{6.16}$$

compared to the time of flight of the measurement ultrasound signal (propagating with $v_{sound} \approx 330\,\mathrm{m/s}$)

$$t_{measure} = s/v_{sound} = 20/330 \approx 6.1 \cdot 10^{-2} s \tag{6.17}$$

$$\frac{t_{start}}{t_{measure}} \leq 1.11 \cdot 10^{-6} \tag{6.18}$$

6.5 Receivers

The receivers consist of a "detect start signal device" and an ultrasound receiver. When the start signal is received (in one of the different ways described above) a clock starts counting. The clock can for example be a simple microprocessor with an integrated timer and sufficient clock frequency. The position accuracy is very much related to the clock speed.

Considering the speed of sound in air the following relation is obtained

$$d_{acc} = v_{sound} \cdot t_{clock} \tag{6.19}$$

which states that for an ideal situation, when only the clock speed is affecting the measurement, a clock speed of 1 MHz and $v_{sound} = 330\,\mathrm{m/s}$ gives a maximum accuracy of $d_{acc} = 3.4 \cdot 10^{-4}\,\mathrm{m}$=0.34 mm for a single distance measurement. In reality, several factors affect the measurement and an error in each measurement can during position calculation give a resulting error that is considerably larger than the errors themselves.

6.6 Position Calculation

When a measurement cycle is complete and the distance measurements from all transmitters to all receivers are done, the position is to be calculated. Here a cartesian coordinate system fixed to the ground is used to express the position. Of course any other coordinate system can be used, if for some reason it should be preferable.

When all the receivers have acquired a value corresponding to the measured distance from the transmitter to each receiver, the measurement values are passed on to the "position calculation system" which mainly consists of a microprocessor or similar capable of doing the required calculations fast enough.

What calculations are required then? In this case three receivers and one transmitter is used to illustrate the principle. Let $r_i = \begin{bmatrix} x_i & y_i & z_i \end{bmatrix}^T$ be the position vector of the i:th receiver station and $r_v = \begin{bmatrix} x & y & z \end{bmatrix}^T$ be the vehicle position vector in three dimensions. The distance R_i between the vehicle and the i:th station s_i can be expressed as

$$R_i = \left((x - x_i)^2 + (y - y_i)^2 + (z - z_i)^2\right)^{1/2} \qquad i = 1, 2, 3 \tag{6.20}$$

for which a solution for $r_v = \begin{bmatrix} x & y & z \end{bmatrix}^T$ is wanted.

A set of three equations of the above form is available, one for each distance measured. Geometrically this is equivalent of drawing a sphere with radius R_i around each measuring station.

To solve this it is necessary to calculate the intersection of the three spheres. This can be done in several ways, for example by expanding the above equation in a Taylor series and in that way linearizing around a point close enough to the actual position. The linearized equation can be solved and the solution can be an estimate for r_v and used as the new linearization point. By repeating this an

iterative method for position estimation is obtained. However, this method has several drawbacks: An initial guess is required, convergence is not generally assured and the iterative nature of the method makes it computationally demanding [15]. In this case the biggest problem is likely to be the large computation time — a faster and more efficient method is needed.

In [15] a computationally efficient solution is proposed and its performance is discussed. In the following a brief outline of the method will be given together with a discussion of its advantages and drawbacks in this application.

Horizontal Position

The initial set of equations can be transformed into a set that can be solved explicitly. First an expression for the horizontal position is derived. Squaring (6.20) gives

$$R_i^2 = S_i^2 - 2x_i x - 2y_i y - 2z_i z + x^2 + y^2 + z^2, \qquad i = 1, 2, 3 \tag{6.21}$$

where

$$S_i^2 = x_i^2 + y_i^2 + z_i^2 \tag{6.22}$$

If R_1^2 is subtracted from R_i^2

$$R_i^2 - R_1^2 = S_i^2 - S_1^2 - 2x_{i1}x - 2y_{i1}y - 2z_{i1}z, \qquad i = 2, 3 \tag{6.23}$$

where

$$\begin{aligned} x_{i1} &= x_i - x_1 \\ y_{i1} &= y_i - y_1 \\ z_{i1} &= z_i - z_1 \end{aligned}$$

Now a set of two equations is acquired (since one is evaluated to zero during the subtraction above). Writing this in matrix form gives

$$\begin{aligned} \mathbf{W}\mathbf{r_h} &= \boldsymbol{\beta} - \mathbf{d}z \\ \boldsymbol{\beta} &= \begin{bmatrix} \beta_2^2 \\ \beta_3^2 \end{bmatrix} \qquad \mathbf{r_h} = \begin{bmatrix} x \\ y \end{bmatrix} \\ \mathbf{d} &= \begin{bmatrix} z_{21} \\ z_{31} \end{bmatrix} \qquad \mathbf{W} = \begin{bmatrix} x_{21} & y_{21} \\ x_{31} & y_{31} \end{bmatrix} \end{aligned}$$

$$\beta_i^2 = (R_1^2 - R_i^2 - S_1^2 + S_i^2)/2, \qquad i = 2, 3$$

Finally, if $\mathbf{W}$ is nonsingular, the horizontal position vector can be expressed as

$$\mathbf{r_h} = \mathbf{W}^{-1}(\boldsymbol{\beta} - \mathbf{d}z) \tag{6.24}$$

r_h is here a function of z and the constant (known) positions of the receiver stations.

The only case when W is singular is when all three stations are located on the same line, and in that case the vectors $\begin{bmatrix} x_{21} & x_{31} \end{bmatrix}^T$ and $\begin{bmatrix} y_{21} & y_{31} \end{bmatrix}^T$ of $\mathbf{W}$ are linearly dependent causing the determinant of $\mathbf{W}$ to be zero.

Vertical Position

Equation (6.21) with $i = 1$ can be rewritten in the form

$$R_1^2 = S_1^2 - 2\mathbf{r_{h1}^T r_h} - 2z_1 z + \mathbf{r_h^T r_h} + z^2 \tag{6.25}$$

$$\mathbf{r_{h1}} = \begin{bmatrix} x_1 & y_1 \end{bmatrix}^T$$

Substituting (6.24) in (6.25) the vertical position of the vehicle can be seen as a quadratic expression

$$az^2 + bz + c = 0 \tag{6.26}$$

where

$$a = 1 + \mathbf{d^T W^{-T} W^{-1} d} \tag{6.27}$$

$$b = 2\mathbf{r_{h1}^T W^{-1} d} - 2z_1 - 2\mathbf{d^T W^{-T} W^{-1}}\boldsymbol{\beta} \tag{6.28}$$

$$c = S_1^2 - R_1^2 + \boldsymbol{\beta}^{\boldsymbol{T}}\mathbf{W^{-T} W^{-1}}\boldsymbol{\beta} - 2\mathbf{r_{h1}^T W^{-1}}\boldsymbol{\beta} \tag{6.29}$$

The height of the vehicle can be calculated using the normal solution for an equation of second degree.

$$z = (-b \pm (b^2 - 4ac)^{1/2})/2a \tag{6.30}$$

The solution gives two symmetric points, one on each side of the plane of the stations. In this case the positive sign should be used, assuming the vehicle is always located at a higher altitude than any of the receiver stations. Combining the expressions for vertical position (6.30) and horizontal position (6.24) gives an expression for the the three dimensional position vector $\mathbf{r_v}$.

$$\mathbf{r_v} = \begin{bmatrix} x \\ y \\ z \end{bmatrix} = \begin{bmatrix} \mathbf{W^{-1}}\beta \\ 0 \end{bmatrix} + \begin{bmatrix} -\mathbf{W^{-1}d} \\ 1 \end{bmatrix} (-b + (b^2 - 4ac)^{1/2})/2a \tag{6.31}$$

Efficient Solution

Noticing that $\boldsymbol{W}$, $\boldsymbol{d}$ and $\boldsymbol{r_{h1}}$ depend on the coordinates of the measuring stations only and that $\boldsymbol{\beta}$ depends on both the distance measurements and the station positions, $\boldsymbol{\beta}$ can be rewritten as

$$\boldsymbol{\beta} = (1/2)(\boldsymbol{\rho} - \boldsymbol{\delta}) \tag{6.32}$$

where $\boldsymbol{\rho} = \begin{bmatrix} \rho_2^2 & \rho_3^2 \end{bmatrix}^T$, $\boldsymbol{\delta} = \begin{bmatrix} \delta_2^2 & \delta_3^2 \end{bmatrix}^T$

$$\rho_i^2 = R_1^2 - R_i^2, \qquad i = 2, 3$$
$$\delta_i^2 = S_1^2 - S_i^2, \qquad i = 2, 3$$

Substituting (6.32) in (6.31) together with some algebraic operations gives an expression for the three dimensional position vector

$$\boldsymbol{r_v} = \boldsymbol{f(r)} = \boldsymbol{\Lambda u} + \boldsymbol{\mu}(\boldsymbol{\xi^T v})^{1/2} \tag{6.33}$$

where $\mathbf{r}$ is the range measurement array, $\mathbf{r} = \begin{bmatrix} R_1 & R_2 & R_3 \end{bmatrix}^T$. The details are not shown here, but can be found in [15]. However, the point is that only the vector $\mathbf{u}$ and $\mathbf{v}$ involve the distance measurement. All other vectors $\boldsymbol{\Lambda}$, $\boldsymbol{\mu}$ and $\boldsymbol{\xi}$, depend only on the (constant) coordinates of the measuring stations and only need to be calculated once.

6.7 Performance Analysis

When performing distance measurements, the result is likely to contain an error. Assume a random error δR_i is added to the actual distance R_{i0}. The measured distance can then be written

$$\mathbf{r} = \mathbf{r_0} + \delta\mathbf{r} \tag{6.34}$$

where $\mathbf{r_0} = \begin{bmatrix} R_{10} & R_{20} & R_{30} \end{bmatrix}^{\mathbf{T}}$ and $\delta\mathbf{r} = \begin{bmatrix} \delta R_1 & \delta R_2 & \delta R_3 \end{bmatrix}^T$. The errors are assumed to have a mean value of zero, that is

$$E\{\delta\mathbf{r}\} = \mathbf{0} \tag{6.35}$$

where E is the expected value operation. The errors in distance measurement data will result in an error in the calculated position according to

$$\delta\mathbf{r_v} = \mathbf{r_v} - \mathbf{r_{v0}} \tag{6.36}$$

where $\mathbf{r_{v0}} = \mathbf{f}(\mathbf{r_0})$ is the actual position of the vehicle and $\delta\mathbf{r_v} = \begin{bmatrix} \delta x & \delta y & \delta z \end{bmatrix}^T$.

The function relating the distance measurements to the calculated three dimensional position is nonlinear, hence $E\{\delta\mathbf{r_v}\} \neq 0$ and the position estimate will be biased. So even though the position measurement errors have zero mean value, the position estimate will be biased. In [15] an expression for the bias and the covariance matrix are derived, which will not be shown here.

The performance of the algorithm is affected by the distance measurement errors and by the geometrical arrangement of the measurement stations and also the position of the vehicle relative to the measurement stations. The Dilution Of Precision (DOP) is caused by the geometry of the measurement station and can be defined as a measurement of the ranging error amplification when the position of the vehicle is calculated. If the distance measurement errors are assumed to be

uncorrelated with the same variance σ^2, the following performance indices can be defined

$$GDOP = \frac{\sqrt{\sigma_x^2 + \sigma_y^2 + \sigma_z^2}}{\sigma} \tag{6.37}$$

$$HDOP = \frac{\sqrt{\sigma_x^2 + \sigma_y^2}}{\sigma} \tag{6.38}$$

$$VDOP = \frac{\sqrt{\sigma_z^2}}{\sigma} \tag{6.39}$$

where geometric DOP (GDOP) is a general performance index, horizontal DOP (HDOP) is the performance index for the XY-plane and vertical DOP (VDOP) is the performance index for the vertical position. The VDOP can be rewritten as $\sigma_z = (VDOP) \cdot \sigma$, where σ_z is the standard deviation of the vertical position error.

A similar calculation can be done for the bias which gives that the position estimation systematic errors can be expressed as

$$b_x = B_x\sigma^2 \qquad b_y = B_y\sigma^2 \qquad b_z = B_z\sigma^2 \tag{6.40}$$

where B_x, B_y and B_z are geometric factors expressing the effect of system nonlinearities and can be referred to as normalized bias. The total bias b_t and the total normalized bias B_t can be defined as

$$b_t = B_t\sigma^2 \qquad B_t = \sqrt{b_x^2 + b_y^2 + b_z^2} \tag{6.41}$$

The conclusion is that standard deviation of the position estimation error is proportional to the distance measurement errors whereas the position estimation bias is proportional to the square of the distance measurement errors.

6.8 Performance Evaluation

The measurement stations are placed in an equilateral triangle inscribed in a circle with radius l and the origin of the coordinate system in the center of the circle. The location vectors of the measurement stations are thus $\mathbf{r_{h1}} = \left[-l\sqrt{3}/2, -l/2\right]^T$, $\mathbf{r_{h2}} = \left[0, l\right]^T$ and $\mathbf{r_{h3}} = \left[l\sqrt{3}/2, -l/2\right]^T$. In [15] simulations have been done showing the different DOP for various positions. The conlusion is that for Horisontal DOP, HDOP, the distance from the center of the stations is the only thing affecting the measurements. The Vertical DOP, VDOP, is affected by both the distance and the relative position of the vehicle compared to the measurement stations, however the relative position has reduced influence for distances far from the center. While the HDOP is approximately a linear function of the distance from the center, the VDOP shows a slightly quadratic function.

6.9 Conclusion

The low speed of sound is both the main advantage and the main problem with this method. The low speed makes it possible to measure the time of flight in a simple way but for example the temperature of the air have a great impact on the measured result. Thus the performance of this system is greatly dependant on the ability to estimate the speed of sound in air. Inability to accurately estimate the speed of sound strongly decreases the measurement accuracy of the system.

There may also be disturbances caused by noise from the propeller and motor which may disturb the measurement ultrasound signals. The effect of ultra sound on humans and other organisms are another concern with this method. For example dogs and other animals can hear ultra sound. The method also relies on ultra sonic transmitters with a wide radiation pattern, without this the receivers may not pick up the measurement signal if the vehicle is tilted.

Chapter 7

Global Positioning System

The Global Positioning System (GPS) is described in [13, 17, 18].

7.1 System Overview

The GPS is a worldwide, satellite based positioning system operated by the U.S. Government. The system consists of 24 satellites in orbit together with a few extra "spare" satellites. The 24 satellites are placed four and four in each of six orbital planes, orbiting the earth at an altitude of 20,051 km and a 12-hour period. The system is designed so that at least four satellites always are within the line of sight at any position on the earth, at any time. The system originally consisted of one military and one civilian part, and a random "disturbance signal" was added to the civilian part in order to decrease accuracy. This disturbance signal was however removed in the year 2000 and today both systems provide nearly the same accuracy. The U.S. Government though has the right to deny users access to the system in certain areas during special circumstances, as for example conflicts. This has so far never happened (June 2005) [18].

7.2 Position Measurement

All GPS satellites have an on-board atomic clock used for the precise timing needed for position calculation. Each satellite broadcasts position data at precisely known times (hence the need for the atomic clock). Each receiver also has a clock and can thereby measure the time at which it receives the signal from the satellite. By calculating the time delay between signal transmission and reception the distance between transmitter and receiver can be measured. Each satellite's position is known so by measuring the distance to three different satellites, the position in three dimensions can be calculated. However the clock in the receiver may be rather simple and not very accurate, so therefore the precise time is also broadcasted together with the position data. Only three satellites are needed for position

calculation and the fourth is used to set the receiver clock. If more than four satellites are available, the position accuracy can be increased.

Orbital Deviations

The satellites may drift slightly in their orbit positions. Fixed ground stations at several locations in the world are used to observe the satellites and measure any deviation from the predicted orbit. These deviations are sent to a "master controller" which in turn transmits a message to each satellite telling it how much it is deviating from its predicted orbit and also providing time corrections to the atomic clock in the satellite (actually, the atomic clocks in the satellites are affected by relativistic effects and therefore need to be calibrated more often than otherwise). These orbital deviations are passed on in the position data sent to the receivers for a more accurate position calculation.

Disturbances

A number of things affect the achieved accuracy in a position measurement, for example atmospheric conditions, solar flux density, the geometry of the satellite constellation at that time, position computation algorithm and also the receiver area geometry (buildings may cause multi path disturbances) to mention a few. In [17] the different kind of disturbances are described in detail.

7.3 Improvements and Performance

Improvements

One way to improve GPS performance is Differential GPS (DGPS), which is based on the following principle: A GPS receiver is placed at a known location and the position is measured. The reading from the GPS system is compared with the known position, and the difference is used to derive a correction signal, which can be sent to nearby receivers. The DGPS was invented when there was a disturbance signal added to the civilian GPS signal. By measuring the deviations from a reference position the (partly constant) error signal could be found. Now when the disturbance signal is removed, the DGPS can be used to measure for example atmospheric disturbances and correct for these. With DGPS and/or other methods for improvements sub-centimetre accuracy can be achieved [17].

Another method for improvement based on the same principle as DGPS is the Wide Area Augmentation System (WAAS). It uses a combination of satellites and ground based stations to send correction signals to GPS receivers, as well as providing integrity information for each satellite's signal [17].

Accuracy

In [17] accuracy tests have been done in June 2000 (today better performance may be expected) for the so called SPS (Standard Positioning Service). An average

accuracy of about 8 meters in horizontal position and 16 meters in vertical position respectively has been achieved.

Update Rate

The update rate of a standard GPS receiver is about 1 Hz, i.e., one position update every second. However, there are high end models that can give a position update rate of up to 100 Hz, such as for example the JNS-100 from Javad Navigation Systems [10]. However additional signal treatment such as mean value or low pass filtering may be necessary, thus decreasing the update rate. This receiver is using a combination of the American GPS system and also the Russian GPS counterpart, the GLONASS system, together with the WAAS. Sub-centimetre accuracy is claimed during acceptable conditions.

7.4 Conclusion

For this application a position in global coordinates (as produced by the GPS) is not necessary, the only relevant thing is to detect a deviation from a reference position. The GPS positioning method also incorporates dependence to an external system (that can not be controlled), which affects the robustness of the whole UAV system. The possibility of GPS failure or bad reception must be taken into account, and for cases like this a back-up system may be necessary. The GPS receiver and a possible back-up system adds extra weight to the vehicle, and for the prototype system with very limited lift capacity this is not an option.

Although it may be possible to achieve acceptable accuracy and update rate with a general GPS system this is likely to require complicated (and heavy) receiver equipment, which makes it impossible to use in reality. A small and low-weight GPS receiver is not likely to be able to give sufficient position accuracy. The GPS system also does not generally work indoors, which is one of the requirements for the positioning system.

Chapter 8

Evaluation System

In this chapter a description of the evaluation system is given. At first an overall system description is given, followed by a detailed description of the different parts of the system. In Section 8.3 the measurement process is described, followed by a discussion of sources of errors in Section 8.4 and an error analysis in Section 8.5. Finally in Section 8.6 the tests and actual measurements are described.

8.1 System Overview

An evaluation system has been designed and implemented in order to evaluate the approach with PSD sensor described in Chapter 4. The evaluation system was constructed with very simple means: Based on an old slide projector AGFACOLOR 250, a few LEDs with different wavelengths, an AVR ATmega16 8-bit RISC microcontroller and a Position Sensing Detector (PSD). A schematic drawing of the experimental set-up is shown in Figure 8.1 and each of the subsystems will be described in detail in the following sections.

Short Description of the Evaluation System

This is a very brief description of the evaluation system. The principle schematic in Figure 8.1 may be helpful when reading this description. An output signal from the microcontroller controls the LEDs. The LEDs are turned on one at a time, the objective is collecting the light from the active LED (and all other incident light) onto the surface of the PSD. The optical filter removes the visible wavelengths (below 750 nm). In an ideal situation the only light on the PSD surface would now be a projection of the active LED into a single point. The PSD is connected to the evaluation board which produces two voltages for x- and y-position of the light spot. These voltages are put into a difference amplifier in order to make them suitable for the analogue to digital converter. The microcontroller reads the output from the difference amplifier via the built-in analogue to digital converter, calculates necessary information and transmits the result over the serial UART

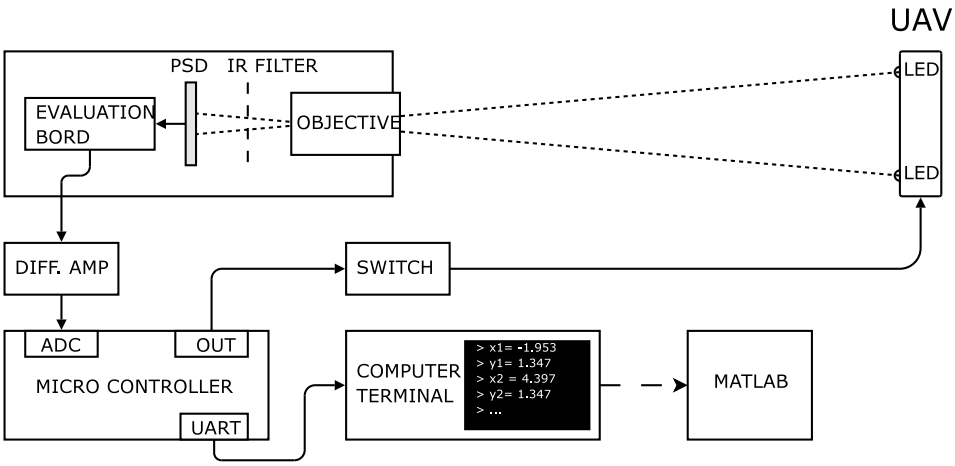

Figure 8.1. Principle schematic of the evaluation system.

to the computer terminal. After all the necessary calculations are made, the measurement sequence starts over from the beginning.

8.2 System Description

In this section a description of each of the subsystems and components in the evaluation system will be given.

Projector

The reason for choosing the slide projector was that it had a (presumably) good enough lens and also was easy to experiment with. Keeping the low cost goal in mind, it was also acquired for free. The alternative would have been to have a "box" built with the PSD sensor mounted inside and fitted with for example the standard so called C-mount for mounting an objective on it. This would of course give better opportunities to adjust the properties of the optical system, such as focal distance and field of view of the system. However, for evaluation of system performance this was not considered necessary, and thus a simple, low cost test system was built with simple means. In Figure 8.2 a picture of the unmodified projector is shown.

Light Emitting Diodes (LEDs)

As light sources LEDs in the infrared (IR) spectrum were chosen. The reason for this was partly that a simple IR-pass filter easily could be constructed, but also that the PSD has maximum spectral response for wavelengths around 950 nm. LEDs with a wavelength of 880 nm were chosen because of being commercially

Figure 8.2. The unmodified slide projector.

available and working well with the conditions stated above. The LEDs have an intensity of 432 mW/sr (sr = steradian, a solid angle measurement (cone), defined in [16]) and a rather narrow radiation pattern, ± 10°. At a distance of 10 metres this gives radiation area with radius of about 1.8 m. At later experiment this has shown to be rather small because the intensity in the outer parts of the circle is a lot lower than at the centre. Thus the effective and useable circle in fact has a smaller radius. However, the narrow LEDs were uses because of the high intensity at the radiated area. A wider radiation pattern requires more power to keep a sufficiently high intensity over the whole area. In order to achieve stronger light intensity laser diodes may be used, but this has however not been tested. The system has also been tested with wavelengths in the visual spectrum.

Objective

The projector has an objective with focal distance $f = 90\,\text{mm}$ and an aperture of $N = f/2.5 = 36\,\text{mm}$. Using (4.11), (4.12) and (4.13) in Section 4.3.2, at a distance of $u = 10\,\text{m}$ and a circle of confusion of $C = 0.022\,\text{mm}$ (lowest resolution due to other errors, see Section 8.5) this gives a depth of field as described in (8.2).

$$S = 10.73 \geq DOF \geq R = 9.36 \Rightarrow \tag{8.1}$$
$$T = 1.37m \tag{8.2}$$

However if a circle of confusion of $C = 0.1\,\text{mm}$ is allowed a higher DOF is obtained

$$S = 14.46 \geq DOF \geq R = 7.64 \tag{8.3}$$
$$T = 6.82m \tag{8.4}$$
$$h = 32.4m \tag{8.5}$$

where h is the hyper focal distance. By setting the focus to the hyper focal distance, a DOF of

$$S = h/2 = 16.2m \geq DOF \geq R = \infty \tag{8.6}$$
$$\tag{8.7}$$

is obtained. A circle of confusion of $C = 0.1\,\text{mm}$ may seen much compared to $C = 0.022\,\text{mm}$. But since the output from the PSD is the "centre of gravity" of the incident light, this increased blur is not likely to affect the measurements in any greater way. However, caution should be taken here and the light spot should always be kept as focused as possible. An unfocused light spot causes problems with stray light and decreases measurement accuracy [21].

The FOV can relatively easy be changed by either adjusting the distance between the PSD and the objective or change the size of the PSD. In case a too small detector is chosen the light that goes outside the PSD is simply ignored, the result being a smaller FOV. This is illustrated in Section 4.3.2. The FOV for the evaluation system has been determined with the help of (4.9) and (4.10) to

$$FOV = 2 \cdot arctan(\frac{h}{a_1}) \approx 5^o \tag{8.8}$$

This is course too low for a real measurement system, however the low FOV was accepted because of practical issues when mounting the PSD sensor.

Optical Filter

The optical filter is made of a piece of exposed negative film. The negative film is used during the development process of photographic pictures, and is supposed to limit what wavelengths that are allowed to pass through the negative and reach the light sensitive photographic paper. The colours in the negative film are the opposite of the photograph. When lit by white light (containing all colours) some wavelengths are absorbed in the negative and the result is that those colours do not reach the photographic paper. Thus, if the negative of a white photo (or a piece of film that have been exposed to light, from for example the end of the film) is used, no visible light will be let through. Of course this is for the ideal case, in reality some light will pass through, however strongly reduced. An approximative absorption spectrum for negative film is shown in Figure 8.3(a) together with the spectral response of the PSD is shown in Figure 8.3(b).

As seen in Figure 8.3(a) the negative film has a fairly high transmission for long wavelengths, which may let unwanted light through and can eventually interfere with the measurement. However, if the response spectrum for the PSD sensor is combined with that of the negative film the combined spectrum creates a band pass filter. Both the transmission curve of the negative film and the spectral response of the PSD are shown in Figure 8.2

PSD

Specific information about the PSD is taken from the data sheet [22] supplied by Hamamatsu Photonics Inc. together with the PSD.

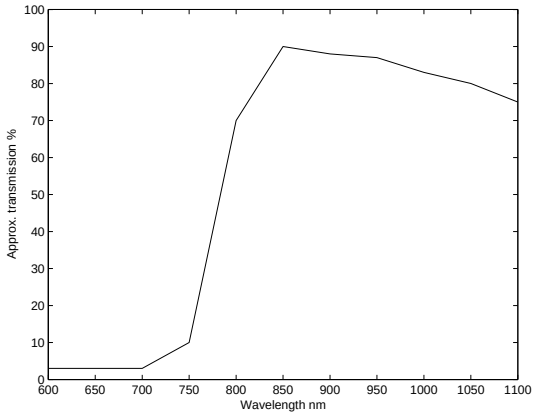

(a) Approximate transmission spectrum of negative film, [29].

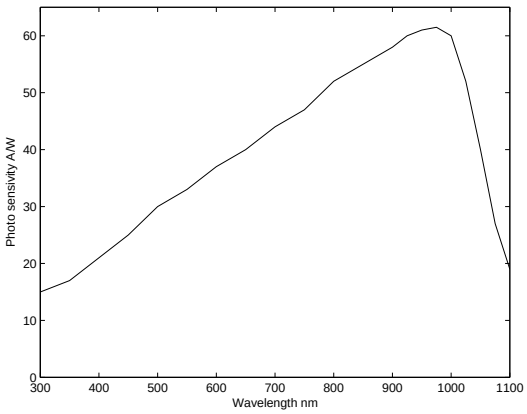

(b) Spectral Response for PSD, [22].

Figure 8.3. Transmission properties of negative film and PSD.

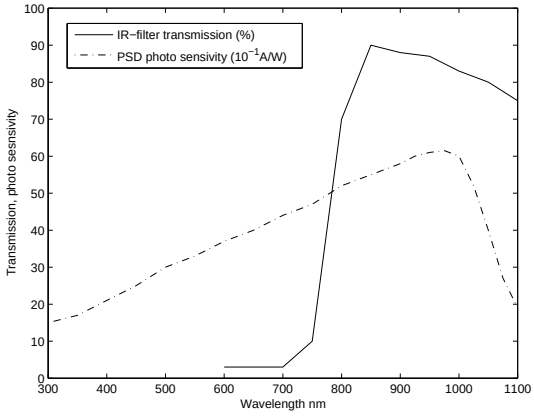

Figure 8.4. Spectral response of PSD combined with spectral transmission of negative film.

An improved tetra lateral (pin cushion-type) PSD was chosen, partly because the ten times difference in price, but also because the slightly decreased linearity compared to the duo lateral type PSD is negligible [22] and for the evaluation system the properties of the tetra lateral PSD were considered good enough. The different types of PSDs are described in Section 4.

Evaluation Board

An evaluation board supplied by the manufacturer of the PSD, Hamamatsu Photonics Inc., was used in order to start measurement in an easy way. The evaluation board is supplied with $\pm 15\,\mathrm{V}$ and produces an output proportional to the two dimensional position of an incident light spot. The output voltages can be adjusted to be $1\,\mathrm{V/mm}$ in both x- and y-directions, starting with origin in the middle of the sensor. A negative position value is thus represented by a negative voltage and vice versa, the output is a voltage between $\pm 4.5\,\mathrm{V}$, one voltage for each direction.

Difference Amplifier

In order to be able to use the built in Analogue to Digital Converter (ADC) in the microcontroller, the voltage input has to be between $0\,\mathrm{V}$ and $4.5\,\mathrm{V}$. A difference amplifier was constructed to achieve this, see schematic in Figure 8.5.

The output from the difference amplifier is described in (8.9). A voltage of $4.5\,\mathrm{V}$ is added to the input and the result is then multiplied by $\frac{1}{2}$, thus an input of -4.5 V corresponds to $0\,\mathrm{V}$ output and an input of $+4.5\,\mathrm{V}$ corresponds to $4.5\,\mathrm{V}$.

$$V_{ADC} = \big(V_{IN} - (-4.5)\big)\frac{R_2}{R_1} = (V_{IN} + 4.5)\frac{1}{2} \tag{8.9}$$

Some inaccuracies in the offset voltage exist, however since these are assumed

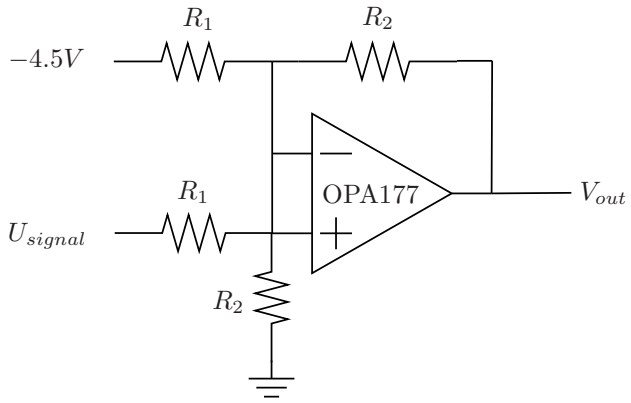

Figure 8.5. Electrical schematic of the difference amplifier.

constant the biggest error is likely to be disturbances in the cables and also from non-linearities in the amplification. These disturbances will not be studied in further detail.

Analogue to Digital Converter and microcontroller

This section is written using data from the AVR and STK500 data sheets, [4] and [5].

The Atmel ATmega16 AVR 8 bit RISC microcontroller was used. The ATmega16 has a built in 10-bit ADC and was also supplied together with a STK500 Starter Kit and Development System to give a quick start for development. The STK500 handles supportive functions for the AVR, such as clock frequency generation, voltage reference for ADC and is also equipped with LEDs and switches for testing purposes. The AVR is programmed via the RS232 serial standard interface through the serial port of a computer (in this case actually a serial port to USB-adapter). The program code was written in C and compiled using Atmel's development tool AVR Studio 4 together with the open source WinAVR tool.

The Atmel AVR microcontroller was chosen in favour of the Microchip PIC microcontroller, mainly because the better development environment for programming and debugging.

The built in ADC uses a conversion method of successive approximation and it takes approximately 13 ADC clock cycles for a typical conversion. The first conversion takes 25 ADC clock cycles because the analogue circuitry needs to be initialised. The ADC clock runs with a prescaler from the system clock and can handle frequencies between 50-200 kHz. A system clock frequency of 3.686 MHz and a prescaler of 32 gives ADC frequency of $f_{ADC} \approx$115 kHz and a typical conversion time of $t_{ADC} = \frac{13}{(3.686 \cdot 10^6/32)} \approx 11.3\,\mu$s. The ADC input on the microcontroller needs to be connected to a low impedance source in order or produce a good result. This is however not a problem since it is connected directly to the output of the

OP-amplifier included in the difference amplifier, which has an output impedance in the order of 10 Ω.

UART

The microcontroller communicates with the serial interface standard UART (Universal Asynchronous Receive Transmit). The communication is done over the serial port of a computer, and the result is printed in a terminal window using the ASCII standard. A problem here is that the AVR microcontroller only can transmit one byte at a time, so in order to transmit for example position data the float position data has to be converted to a series of integers that then can be converted to ASCII and finally transmitted one by one.

Matlab

By formatting the data printed in the terminal window in a suitable way and then saving it to a file, it could be imported to Matlab for post processing or analysis as well as for plotting.

8.3 Measuring Sequence

In this section a position measurement it is described. A flowchart explains the process, see Figure 8.6. Below, every box in the flowchart is explained in detail. Keeping the principle schematic of the system, shown in Figure 8.1, in mind may be of help.

Initialisation

Initialisation of the microcontroller: Setting variables, setting output/input registers, configuring interrupts and setting parameters for UART.

Turn on LED

Writing to the AVR output register activates LED1. A certain rise time is needed to let the LED achieve full power and it is given by the following equation

$$t_{rise} = t_{AVR} + t_{ULN} + t_{LED} = 0 + 250 + 500 = 750ns = 0.75\mu s \tag{8.10}$$

where t_{AVR} is the delay in the microcontroller, t_{ULN} the delay in the LED switch and t_{LED} is the rise time needed for the LED to go from 10% to 90% intensity. The delay times are taken from the datasheets for the different components: [4], [14] and [28]. Also some time is needed for the PSD, evaluation board and difference amplifier to register a stable value. This time can be calculated as

$$t_{response} = t_{PSD} + t_{DIFF} = 30 + 15 = 45\mu s \tag{8.11}$$

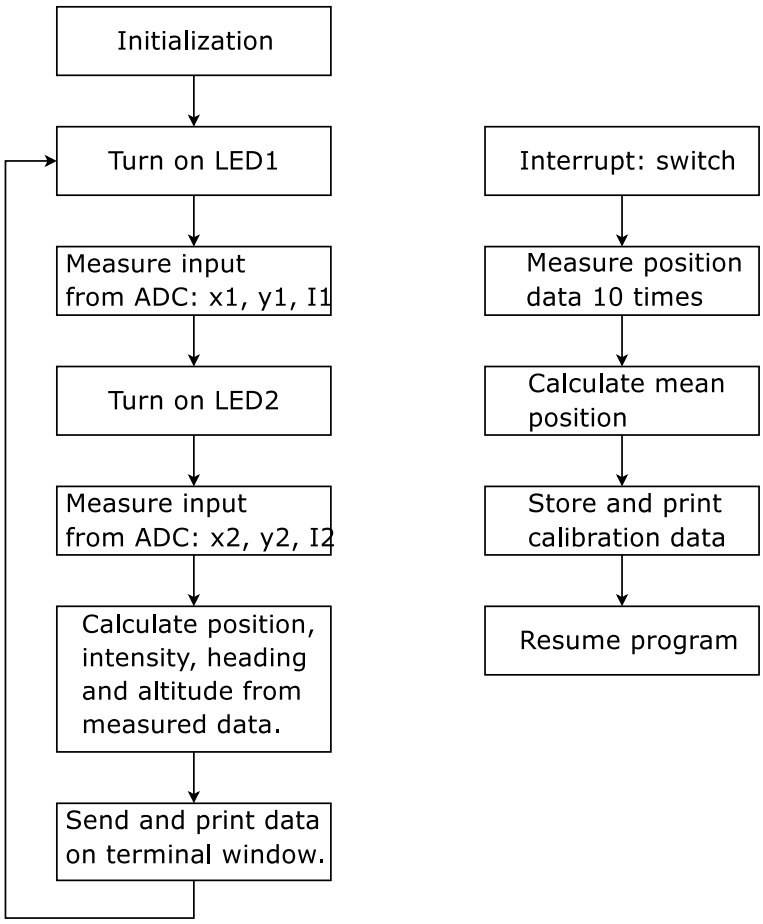

Figure 8.6. Flowchart for position measurement. To the left: Position measurement loop. Right: interrupt routine used for setting origin of measurement coordinate system.

Here t_{PSD} is the time delay until a signal output from the evaluation board is measured. t_{DIFF} is calculated using the slew-rate. Maximum slew-rate $= 0.3\,\mathrm{V}/\mu\mathrm{s}$ $\Rightarrow$ maximum rise time $t_{r,OP} = 4.5/0.3 = 15\,\mu\mathrm{s}$.

So from the point when the microprocessor wants to turn on the LED until there is a reliable value to read with the ADC, there is an approximative maximum delay of $t_{DELAY,MAX} = t_{rise} + t_{response} \approx 46\,\mu\mathrm{s}$. At the used frequency of $f_{AVR} = 3.686\,\mathrm{MHz}$ this means that $t_{DELAY,MAX}/t_{cycle} \approx 17$ clock cycles.

The final delay during AD-conversion does not need to be taken into concern, since the microcontroller waits until the conversion is finished (though it of course affects the measurement time and update rate).

Measure Input

The position of the first LED is measured by sampling the position data output from the PSD. The sampled position signal corresponds to a raw value and will be converted to position data later on. The AVR has 8 different inputs to the ADC, but only one conversion can be done at a time. The signals for x-position, y-position and intensity are all connected to different inputs and sampled one at a time. The intensity signal is an output from the evaluation board and is a measure of the amount of light that hits the sensor. To compensate for different light conditions, a number of resistors and capacitors on the evaluation board can be adjusted and thereby adjust the sensitivity of the sensor.

When the three signals have been sampled the next LED is turned on and the process is repeated. In the evaluation system only two LEDs are used, but there are no difficulties in increasing this to several more LEDs. The only problem is the increased loop time and in turn reduced update frequency.

Calculate Position, Intensity, Heading and Altitude

The input data need to be converted from raw values to input voltages (which corresponds to a sensor position). This is done using (8.12) given in [4], where V_{in} is the input voltage, ADC is the integer value read by the ADC and V_{REF} is the reference voltage, in this case 4.5 V.

$$ADC = \frac{V_{IN} \cdot 1024}{V_{REF}} \tag{8.12}$$

When the sampling process is complete the position is to be calculated. However, in order to calculate the position the distance between sensor and vehicle is needed. Since the LEDs are placed on known locations (with a known distance between them) the distance can be estimated by using the measurement and the known distance between the LEDs in the lens formula.

The heading is calculated using (8.26), and the intensity is simply represented by the read voltage value.

Print Data

Data are sent over the UART link and printed on the computer terminal.

8.4 Sources of Errors

In this section the main sources of errors affecting the evaluation system will be described.

ADC

The ADC is using so called single ended inputs, which means that the signal cable is connected to the input of the ADC and a common ground level is used. This causes some noise to build up in the cable. The use of twisted signal-ground cables would have been able to reduce the disturbances caused by interference from for example other signals.

The resolution of the ADC is 10 bits, which makes a smallest step of

$$V_{ACCURACY} = \frac{4.5}{2^{10}} \approx 4.3945mV \tag{8.13}$$

which corresponds to a theoretical position resolution of approximately 0.0044 mm for the light spot at the detector. Due to the magnifying properties of the objective, the real position resolution will depend on the altitude of the vehicle. Using (4.9), and an altitude of 10 metres the resolution will be

$$\Delta pos = \frac{4.5}{2^{10}} \cdot \frac{a_2}{a_1} \approx 0.44mm \tag{8.14}$$

These steps can also be seen in the position measurement plot shown in Figure 8.9(a).

The ADC has an absolute accuracy less than 2 LSB [4], which is

$$V_{ACCURACY} \cdot 2 \approx 0.0088\,mm \tag{8.15}$$

in position resolution at the sensor. A higher resolution ADC would make a more accurate measurement possible. In order to reduce disturbances during AD conversion, a special noise reduction mode of the microcontroller was used. When put into noise reduction mode the controller stops executing and shut down all its major parts. When the AD conversion is completed an interrupt is given and the microcontroller wakes up and resumes program execution. For further details see the microcontroller technical documentation in [4].

Electrical Noise

The cables used in the evaluation system are mainly unshielded so sometimes a rather high level of electrical noise is present. This varies however depending on cable positions and disturbing signals from surrounding equipment. It is likely that some of the noise is "invisible" due to the low resolution of the ADC. Measures to reduce noise are necessary in future implementations.

Optical Noise

All light (visible and non visible) that hits the PSD sensor affects the measurement. Since the output is the centre of gravity of all incident light, any extra light will cause the position accuracy to deteriorate.

8.5 Error Analysis

In this section an error analysis for the position, altitude and heading calculation has been done.

8.5.1 Numerical Errors

The AVR ATmega16 is programmed using C-code and since the AVR-LIBC library used for compilation currently cannot handle double precision float representation (64 bits), only 32-bit single precision float representation is available. The float is represented using the IEEE standard and in [7] the standard is explained. The smallest possible number that can be used in calculations with this standard is

$$\mu = \frac{1}{2} \cdot 2^{-23} = 2^{-24} \approx 5.96 \cdot 10^{-8} \tag{8.16}$$

However in most cases the numerical errors are negligible due to the coarse resolution of the AD converter. The only case when numerical problems arise is during conversion of a float to a series of integers for transmission over UART as described in Section 8.2. By limiting the number of decimals calculated this error can however be avoided.

Sensor Position

What is the maximum accuracy in position calculation for a light spot on the PSD sensor? The position on sensor, P_s is calculated as

$$P_s = \Big(\frac{P_{raw} \cdot V_{ref}}{1024} - \frac{V_{ref}}{2} \Big) \cdot 2 \tag{8.17}$$

where P_{raw} is the position raw data and $V_{ref} = 4.5\,V$ is considered to be exact. The error here is a maximum absolute error of ± 2 (two least significant bits, LSB) in P_{raw}. This makes a constant error over the entire sensor surface. The maximum error can be calculated by considering the smallest steps in position resolution. An input value of $P_{raw} = 512$ corresponds to a position value of $P_s = 0$ (origin of sensor). Thus the position value from

$$P_{raw} = 513 \Leftrightarrow P_{s,resolution} \approx 0.008789mm \tag{8.18}$$

An error due to the conversion from continuous to discrete representation is also present with a maximum $\pm$ 0.5 LSB. Together this makes

$$P_s = P_{s0} + \Delta P_s$$

where

$$\Delta P_s = \pm 2.5 \cdot P_{s,resolution} \approx 0.022mm \tag{8.19}$$

Error in Altitude

The altitude is calculated using the position measurement data and thus no further measurement errors are added. The altitude is calculated as

$$h_{alt} = \frac{d_v \cdot a}{\sqrt{(x_2 - x_1)^2 + (y_2 - y_1)^2}} + b \tag{8.20}$$

where a and b are constants from the lens formula and d_v is the distance between LEDs on the vehicle. The constants a and b have been experimentally determined since the lens formula is assuming that just *one* lens is used. However the objective consists of a number of different lenses and these constants are needed to compensate for the difference. In this error estimation these constants are treated as being exact.

An estimate of the maximum error can be calculated as [7]

$$|\Delta f| \leq \sum_{k=1}^{n} \left| \frac{\partial f}{\partial x_k} \Delta x_k \right|$$

together with (8.20) this gives

$$|\Delta h_{alt}| \leq 2 \left| \frac{x_1 - x_2}{((x_2 - x_1)^2 + (y_2 - y_1)^2)^{3/2}} \right| \Delta x + 2 \left| \frac{y_1 - y_2}{((x_2 - x_1)^2 + (y_2 - y_1))^{3/2}} \right| \cdot \Delta y \tag{8.21}$$

where Δx and Δy is the error in sensor position (calculated above as ΔP_s) and x_i, y_i is the measured sensor value. If measurement data of x_1, y_1, x_2 and y_2 are put into (8.21) an error of

$$|\Delta h_{alt}| \leq 100mm \tag{8.22}$$

is obtained.

Error in Position

The position of the vehicle in the air is calculated as

$$P_v = \frac{h_{alt} P_s}{a} - \frac{b P_s}{a} \tag{8.23}$$

and by using (8.21) the following is obtained

$$|\Delta P_v(P_s, h_{alt})| \leq \left| \frac{h - b}{a} \Delta P_s \right| + \left| \frac{P}{a} \Delta h \right| \leq 5mm \tag{8.24}$$

Here values from the previous calculations are used together with $h = 10\,\text{m}$ and $P_s = 4.5$ which is the maximum sensor position, i.e., a position on the edge of the sensor.

Error in Heading

The heading is calculated using only the position on the sensor for two points and then calculating the angle between them, using (8.26). The error in angle is calculated in a rather simple way: The two point used for heading calculation each have an error of ΔP_s. The maximum error occurs if the real points are located as far away as possible from the measured points. As illustrated in Figure 8.7 the error can then be expressed as

$$|\Delta\alpha(d_s)| \leq arctan(\frac{2 \cdot \Delta P_s}{d_s}) \leq 2.5^o \tag{8.25}$$

where d_s is the distance between the two measurement points on the sensor when the altitude is 10 m. As can be seen the heading measurement accuracy decreases as d_s decreases. A decrease in d_s corresponds to an increasing altitude and thus the heading measurement accuracy will increase at high altitudes. This may seem strange at first, but studying Figure 8.7 and considering the case when d_s is small it can be realised that a change in one of the measurement points has a great impact on the heading. If, on the other hand, d_s is large a (relatively) small change in one of the measurement points hardly affect the angle between the two points. The conclusion is that the distance between the light sources on the vehicle should be as large as possible. In the evaluation system the distance is only 60 mm, and an increased distance will result in better accuracy.

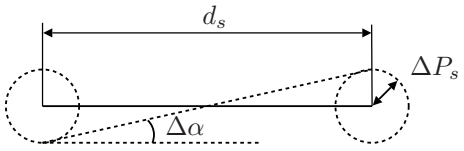

Figure 8.7. Maximum error in heading calculation.

In this section only a basic estimation of the measurement accuracy has been done, and in possible future systems a more thorough investigation is probably needed.

8.6 Testing

In order to test the evaluation system and its performance some tests and experiments have been done. For testing purposes a model was used to simulate the vehicle. The model was very simple and more or less a way to mount the LEDs at a fixed (known) distance from each other and also a way to keep them in the desired position during measurement.

The evaluation system robustness has not been prioritised, and during measurement it is assumed that the vehicle is completely within the FOV of the detector and also that the light intensity at the sensor is “high enough”. Also the lens is

supposed to be focused at the specified distance. If this conditions are not fulfilled different kinds of errors may arise and the measurement data is not reliable.

A method to reduce disturbances from background light and other light sources is to modulate the LED with a certain frequency as described in Section 4.4.1. However, the evaluation board is not designed for use with modulated light sources. To be able to test this a new measurement circuit would have to be designed. This has however not been a priority, partly because it has been possible to significantly decrease and almost completely eliminate the disturbances from surrounding light with the optical filter used.

8.6.1 Position Measurement

The evaluation system was set up and the light sources placed at a distance of about seven meters. The position was measured in darkness in order to exclude disturbances from surrounding light. The vehicle model was placed and kept at a constant position during the measurement. The raw data of the position measurement for coordinate x_1 is shown in Figure 8.8(a). Here the discrete steps of the ADC can be explicitly seen. At this distance the intensity hitting the PSD is rather low. A higher current to the LED would solve this problem. The current used is 0.5 A, but the LED can handle as much as 5 A during short pulses. Increasing the LED power and thus the received intensity would give a higher signal to noise ratio (SNR) and presumably a better position value. This will however not be tested due to lack of time and the fact that the low resolution in ADC would probably make it impossible or very difficult to determine if any improvement has been achieved.

8.6.2 Heading Measurement

The heading is calculated directly from the position measurement data. A slightly modified version of (8.26) is used.

$$\alpha = arctan\Big(\frac{\Delta y}{\Delta x}\Big) \tag{8.26}$$

The modification takes into account some numerical issues to avoid division by zero. It also transforms the resulting angle to a value between 0° and 360° measured from positive x-axis. In Figure 8.10 the heading calculation is shown in detail.

The heading measurement is independent of the altitude of the vehicle, and unlike the position measurement, that greatly depends on the altitude estimation, this signal is a lot more stable in its behaviour. In Figure 8.9(b) heading measurement data are shown.

8.6.3 Altitude Measurement

The distance measurement utilises the fact that the distance between the light sources on the vehicle is known. By comparing the measured distance on the

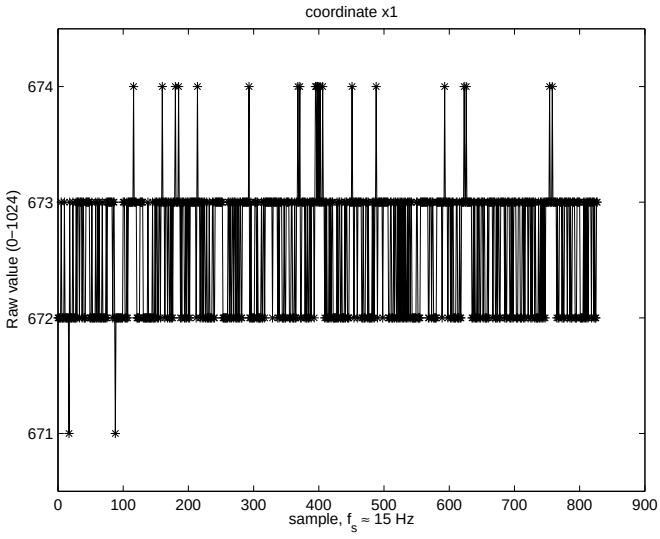

(a) Raw data for position measurement for coordinates x_1.

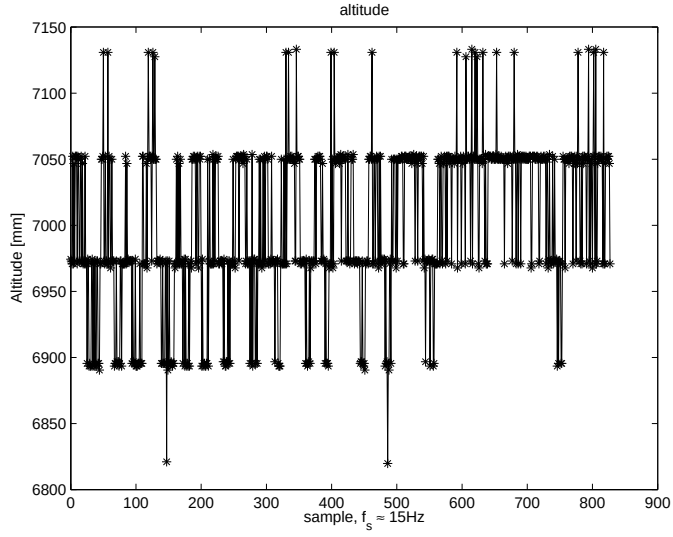

(b) Calculated altitude.

Figure 8.8. Measurement of position and altitude.

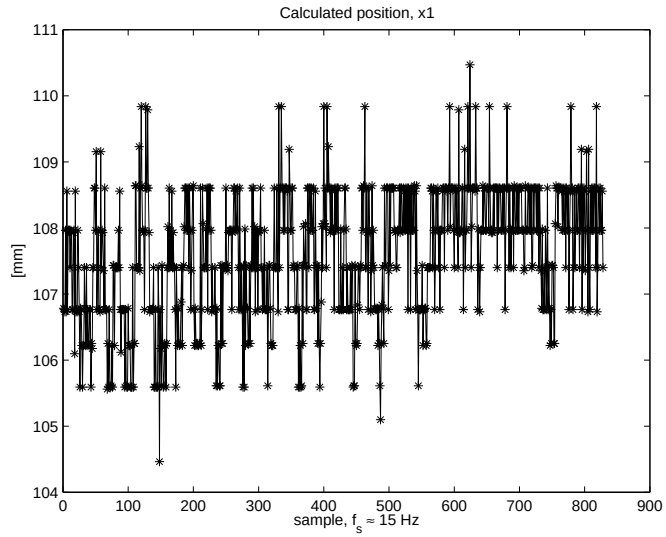

(a) Calculated position using the altitude- and position measurement.

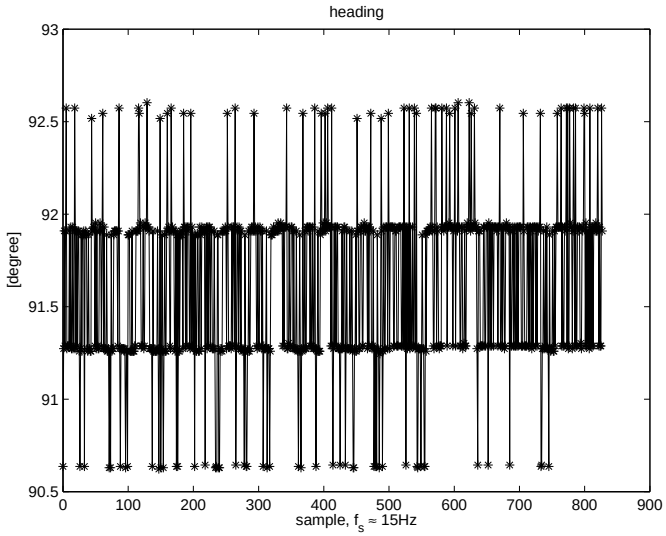

(b) Measured heading.

Figure 8.9. Measurement data for position and heading.

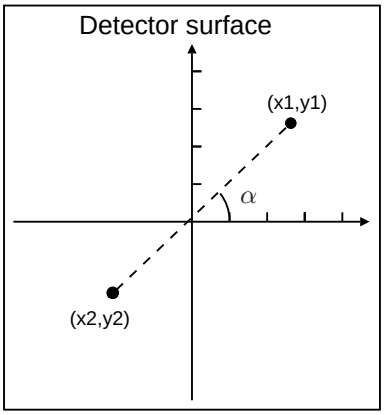

Figure 8.10. Calculation of the vehicle heading.

sensor with the known distance on the vehicle according to (8.20) the altitude can be estimated.

The altitude estimation depends strongly on the orientation of the vehicle. If the vehicle is tilted, the horizontal (projected perpendicular to the optical axis) distance between the light sources will change and the vehicle will appear to be at a higher altitude. A method to compensate for this, either by low-pass filtering the estimation or compensating for a possible tilt of the vehicle is needed in future implementations.

The altitude was estimated from the position readings and by combining position data and altitude an estimate of the position deviation from the origin could be calculated. In Figure 8.8(b) the calculated altitude is shown, and if the position measurement and altitude estimation is combined the position estimation shown in Figure 8.9(a) is acquired.

8.6.4 Update Rate

The update rate is mainly dependent on the calculation speed of the microcontroller. However, since sleep mode is used during AD conversion and thus the controller is idle, this causes a loss of computation time. The transmission of data over UART also takes time. However, here an improvement can be made by using an interrupt instead of keeping the microcontroller waiting for the transmission to complete. The calculation algorithm can probably also be written in a more numerically efficient way. This has however not been a priority and further work remains to be done in this area.

In order to measure the actual update rate the simplest possible method was used: The measurement system was running for a certain time and the number of position calculations were measured.

An update rate of $f_{measure} = 20\,\text{Hz}$ was possible to achieve and still having relatively long delays for rise times of the LEDs and other electronics. This was

done at a clock frequency of $f_{AVR} = 3.686\,\text{MHz}$, but it can be increased to $f_{AVR} = 8\,\text{MHz}$. Due to problems with the UART at this speed, testing this has not been prioritised. However this is not really an issue and can likely be solved relatively easy. A clock frequency of $f_{AVR} = 8\,\text{MHz}$ together with shorter delays would make it possible to achieve a theoretical update speed of $f_{measure} \approx 50\,\text{Hz}$.

Chapter 9

Results and Future Work

In this chapter the results from the theoretical evaluation of technologies (Section 9.1.1) as well as the results from the implemented evaluation system (Section 9.1.2) will be presented. Section 9.2 contains a discussion whether the goals have been achieved and finally in Section 9.3 suggestions for future work and improvements are presented.

9.1 Results

In Chapter 2 five different candidate solutions for position sensing are described: The miniature ILS-system, the Position Sensing Detector (PSD)-system, the Indoor GPS-system from Arc Second, the ultrasound trilateration-system and finally the GPS-system. The results from the investigation of the different technologies are described in the following section.

9.1.1 Evaluation of Technologies

Miniature ILS

The Miniature ILS is an idea for modification of the standard Instrument Landing System (ILS). This solution is based on a supposed educational small scale version of the normal ILS from Park Air Systems [20]. Further investigation has however shown that the supposed educational system was more or less a simulation and not a real small scale ILS system. Since the system could not be used the way intended and the possibilities of building a complete miniature ILS system was rather limited, only a brief discussion of the main principle is given in Section 3. No further investigation of the possibilities of a miniature ILS system has been done, however the method is still considered as an interesting solution.

Position Sensing Detector (PSD)

The PSD system is an optical measurement system. Light sources placed on the vehicle is projected through an objective to the surface of a PSD. The light sources

are controlled by a microcontroller and can be turned on and off at specific times. By using an optical filter a great deal of the surrounding light can be filtered out and the position of the light sources can be read from the PSD output. Using the lens formula and basic trigonometry the vehicle deviation from a reference position can be calculated. An estimate of the altitude as well as heading can also be obtained.

An evaluation system with PSD has been implemented and tested as described in Section 8. The system has proved to have good measurement accuracy and is described further in Section 9.1.2.

Indoor GPS

The Indoor GPS is a complete high accuracy measurement system supplied by Arc Second [1]. The Indoor GPS System has a maximum accuracy better than 1 mm and can be as good as 0.05 mm during optimal conditions. However, the system is mainly intended as an indoor positioning system and although the performance in an outdoor environment is somewhat limited by the sun light, it can still be used outdoors. The system is however not intended for position measurements of an object at such a high altitude as in this application and the performance for situations like this is not known. This solution is also probably not consistent with the low-cost goal of the project, and the high sub-millimtre accuracy is far more than what is necessary.

Trilateration with Ultrasound

This method uses distance calculation with ultrasound. The time of flight for ultrasound pulses between the vehicle and the different ground-based receiver stations are measured. By estimating the speed of sound in air the distances between transmitter and receivers can be calculated. The speed of sound in air is mainly affected by temperature and this is likely to be the major source of error of the system. Also the delay due to the time of flight of the ultra sound measurement signals decreases system performance. A numerically efficient method for solving the distance equations is presented and its performance is discussed.

GPS

The Global Positioning System (GPS) is a satellite based positioning system. The system normally gives an accuracy in the order of a few metres and an update rate of 1 position measurement every second. Different enhancements such as Differential GPS (DGPS) and the WAAS can give a considerably higher accuracy. There are high end GPS-receivers with an accuracy claimed to be below 20 mm and an update rate of 100 Hz. However, this high accuracy receiver likely requires extra receiver equipment and high performance antennas. The major drawback with GPS is that it adds extra weight to the vehicle which may be critical for the prototype system. Using GPS also adds dependancy of an external system that can not be controlled. In case of GPS failure or inability to receive a position signal a back-up system is needed which further increases the weight of the vehicle.

The global coordinates produced by the GPS receiver is also not necessary. In this application only a deviation from a reference position is needed. The GPS system is also not available in an indoor environment which is one of the requirements of the system.

9.1.2 Evaluation System

An evaluation system (described in detail in Section 8) with PSD has been designed and implemented. The evaluation system has been built with simple means and is based on a slide projector. The evaluation system uses a tetra lateral PSD and a microcontroller together with the slide projector and displays the position measurement via the terminal window on a computer. Despite its low budget and simple design good measurement accuracy has been achieved.

A theoretical calculation of the maximum error gives the following results at an altitude of 10 m: An absolute position accuracy of $|\Delta pos| = 5\,\text{mm}$, an accuracy of $|\Delta\alpha| = 2.5\,^o$ in heading and finally an accuracy of $|\Delta alt| = 100\,\text{mm}$ in altitude measurement. The reason for calculating at a distance (altitude) of 10 m is that tests have not been able to be performed at longer distances, and then the theoretical results could not have been verified.

The main sources of errors are disturbances in cables and electronics, shielded cables may remove some of the signal disturbances. A higher resolution in the ADC combined with noise reduction would make it possible to increase accuracy further. The optical disturbances during tests are considered minor due to the indoor, light limited environment.

9.2 Goal

An evaluation system with an accuracy of a few millimetres in the horizontal plane has been constructed. This is better than the goal of 2 cm. However the vertical accuracy is not as good and the goal of 2 cm in vertical accuracy has not been achieved. The heading accuracy of 2° has not been achieved with the evaluation system, however an increased distance between light sources would solve this. The update rate of the system is about the same as stated in the goal, i.e. 10–20 Hz and can probably be increased up to 50 Hz.

9.3 Improvements and Future Work

The major limitations of the evaluation system which needs to be improved are the following:

- Disturbances in cables and electronics. For example shielded signal cables may solve the problem.
- The intensity of the light sources. A wide radiation pattern is wanted so that light can be detected even if the vehicle is tilted, while on the other hand a wider radiation pattern decreases the intensity as the light is spread

over a wider area. An alternative to the LEDs used could be to use the more powerful laser LEDs.

- The resolution of the Analogue to Digital Converter. An ADC with 10-bit was used because of practical reasons, and an increase of the resolution may increase position accuracy. The actual steps of the ADC can be seen during position measurement.
- A modulation of the light source may be necessary to achieve better performance. The modulation makes it possible to filter out constant background light.
- The program code in the microcontroller has not been optimised. The implementation was used during tests and found to work well enough. In order to increase the update rate the code should be optimised regarding speed as well as numerical calculation efficiency. To further increase update rate the clock speed of the microcontroller can be increased up to 8 MHz.
- The lenses used in the projector are made for visible light. For a precision measurementsystem IR-corrected lenses are probably necessary.

The miniature ILS system described in Chapter 3 is also an interesting solution for positioning which may be investigated in future work.

Bibliography

[1] Arc Second. URL: `http://www.arcsecond.com`. Viewed 2006-01-19.

[2] *Error Budget and Specifications*, 2002. Product information from Arc Second.

[3] *Indoor GPS Technology for Metrology*, 2002. Product information from Arc Second.

[4] *8-bit AVR Microcontroller with 16K Bytes In-System Programmable Flash*, 2003. Technical Documentation from Atmel Corporation.

[5] *AVR STK500 - User Guide*, 2004. Technical Documentation from Atmel Corporation.

[6] Projektgrupp Bombus. *Teknisk Dokumentation*, 2005. Project documentation in the course TSRT71, Linköpings Tekniska Högskola.

[7] Lars Eldén and Linde Wittmeyer-Koch. *Numerisk analys - en introduktion*. Studentlitteratur, Lund, third edition, 1996. ISBN 91-44-00172-X.

[8] Mattias Eriksson and Björn Wedell. Performance estimation of a ducted fan UAV. Master's thesis, Linköpings tekniska högskola, 2006. LiTH-ISY-EX-3795-2006.

[9] James E. Hansen and Larry D. Travis. Light scattering in planetary atmospheres. *Space Science Reviews*, 16:527–610, April 1974.

[10] Javad Navigation Systems. URL: `http://www.javad.com`. Viewed 2006-02-24.

[11] Göran Jönsson. *Våglära och Optik*. Teach Support, Lund, second edition, 1999. ISBN 91-972499-0-4.

[12] Seong-Ho Kang and Delbert Tesar. Indoor GPS metrology system with 3D probe for precision applications. Technical report, The University of Texas at Austin, Department of Mechanical Engineering, 2004.

[13] Anthony Lawrence. *Modern Inertial Technology*. Springer-Verlag New York inc, 1998. ISBN 0-387-98507-7.

[14] *GaAIAs Plastic Infrared Emitting Diodes types OP295, OP296, OP297 series*, 1996. Technical Documentation.

[15] Dimitris E. Manolakis. Efficient solution and performace analysis of 3-D position estimation by trilateration. *IEEE Transactions on Aerospace and Electronic Systems*, vol 32(4), October 1996.

[16] Carl Nordling and Jonny Österman. *Physics Handbook for Science and Engineering*. Studentlitteratur, Lund, sixth edition, 1999. ISBN 91-44-00823-6.

[17] US Army Corps of Engineers. *NAVSTAR Global Positioning System Surveying*. Department of the Army, US Army Corps of Engineers, Washington, 2003. URL: `http://www.usace.army.mil/inet/usace-docs/eng-manuals/em1110-1-1003/toc.htm`. Viewed 2006-03-10.

[18] U.S. Department of State. *Fact Sheet*. U.S. Department of State, Bureau of Oceans and International Environmental and Scientific Affairs, 2005. URL: `http://www.state.gov/g/oes/rls/fs/47319.htm`. Viewed 2006-03-10.

[19] Mikael Olofsson. *Basic Telecommunication*. Department of Electrical Engineering, Linköpings universitet, Linköping, 2003.

[20] Park Air Systems. URL: `http://www.parkairsystems.com`. Viewed 2005-10-12.

[21] *The PSD - Position Sensing Detector - User's Manual*, 1996. Printed material supplied by SiTek AB.

[22] *Two-dimensional PSD S5990-01, S5991-01*, 2001. Technical Documentation from Hamamatsu Photonics Inc.

[23] *PSD - Position Sensitive Detector*, 2003. Printed material supplied by Hamamatsu Photonics Norden AB.

[24] Sidney F. Ray. *Applied Photographic Optics - Lenses and optical systems for photography, film, video, electronic and digital imaging*. Focal Press, third edition, 2002. ISBN 0-240-51540-4.

[25] Sitek Electro Optics AB. URL: `http://www.sitek.se`. Viewed 2005-09-22.

[26] Lars Stenberg. The PSD School. Available at URL: `http://www.sitek.se`, 1996.

[27] Paul A. Tipler and Ralph A. Llewellyn. *Modern Physics*. W H Freeman and Company, third edition, 1999. ISBN 1-57259-164-1.

[28] *ULN 2003A: Seven Darlington Arrays*, 2002. Technical Documentation from ST Microelectronics.

[29] URL:`http://www.northcountryradio.com/Articles/irfltr.htm`. Viewed 2005-11-23.

Appendix A

Abbreviations

Abbrevation	**Explanation**
Azimuth	Horisontal angle
ADC	Analogue to Digital Converter
ASCII	American Standard Code for Information Interchange
DGPS	Differential GPS
DOF	Depth Of Field
Elevation	Vertical angle
FOV	Field Of View
GDOP	Geometric Dilution Of Position
GLONASS	Global'naya Navigatsionnaya Sputnikovaya Sistema, GLObal NAvigation Satellite System
GPS	Global Positioning System
HDOP	Horizontal Dilution Of Position
IR	Infrared
LED	Light Emitting Diode
PSD	Position Sensing Detector, analogue detector giving the coordinates of a light spot on its surface.
RISC	Reduced Instruction Set Computer
SNR	Signal to Noise Ratio, a measurement of the relationship between the signal and disturbing noise.
SPS	Standard Positioning Service, a former GPS accuracy level.
UART	Universal Asynchronous Receive Transmit
UV	Ultraviolet
VDOP	Vertical Dilution Of Position
WAAS	Wide Area Augmentation System

This page is intentionally blank.

Appendix B

Speed of Sound

This is a derivation of the speed of sound in air. The speed of sound is used in the trilateration method described in Chapter 6.

Derivation of the Speed of Sound

A soundwave is built up of pressure changes in the air and is a so called longitudinal wave, i.e. the pressure changes arise in the same direction as the direction of propagation for the wave. The following is a brief derivation of the speed of sound in a gas, for details see [11].

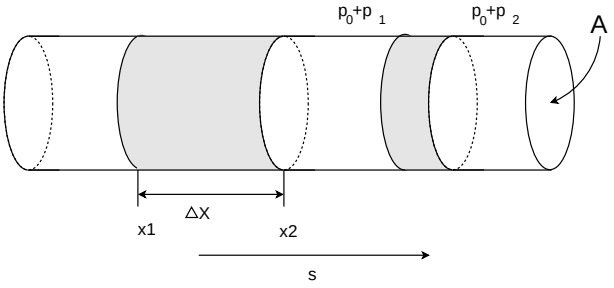

Figure B.1. The unompressed gas in a longitudinal wave at time t_0.

A sinusoidal longitudinal wave is propagating in a tube filled with gas, see Figure B.1. Assume that the wave passes through a volume of gas between x_1 and x_2. At time t_0 the gas is uncompressed, having density ρ, pressure p_0. At a certain time $t_1 > t_0$ the gas volume has been compressed due to the wave and moved a distance s.

The pressure on the left side of the volume is now $p_0 + p_1$ and on the right side $p_0 + p_2$ where p_1 and p_2 is a change in pressure caused by the wave. If the cross section of the tube is A, the net force acting on the gas in the volume will be

$$F = A(p_1 - p_2) \tag{B.1}$$

The mass of the contained gas at t_0 is

$$m = \ \rho \cdot \Delta x \cdot A \tag{B.2}$$

The compressibility coefficient β expresses the change in volume relative to the change in pressure, $\beta = \frac{-1}{V}\frac{\Delta V}{\Delta p}$. If the changes are small β can be defined as

$$\beta = -\frac{1}{V}\frac{\partial V}{\partial p} \tag{B.3}$$

and the pressure change, Δp, can be written as

$$\Delta p = -\frac{1}{\beta}\frac{\partial s}{\partial x} \tag{B.4}$$

When the pressure wave propagates through the tube, the gas is accelerated according to

$$a = \frac{\partial^2 s}{\partial t^2} \tag{B.5}$$

where s is the position of a reference volume in the tube. Using Newton's second law of motion $F = ma$, (B.1), (B.2) and (B.5) gives

$$A(p_1 - p_2) = \rho \Delta x A \frac{\partial^2 s}{\partial t^2} \tag{B.6}$$

$$\frac{-(p_2 - p_1)}{\Delta x} = \rho \frac{\partial^2 s}{\partial t^2} \tag{B.7}$$

for small Δx this can be written as

$$-\frac{\partial p}{\partial x} = \rho \frac{\partial^2 s}{\partial t^2} \tag{B.8}$$

and with (B.4) differentiated and inserted the following is obtained

$$\frac{1}{\beta}\frac{\partial^2 s}{\partial x^2} = \rho \frac{\partial^2 s}{\partial t^2} \tag{B.9}$$

Rewriting this gives

$$\frac{\partial^2 s}{\partial t^2} = \frac{1}{\rho\beta}\frac{\partial^2 s}{\partial x^2} \tag{B.10}$$

Finally, comparing with the general wave equation

$$\frac{\partial^2 s}{\partial t^2} = v^2 \frac{\partial^2 s}{\partial x^2} \tag{B.11}$$

and identifying the coefficients gives the propagation speed of the wave

$$v = \frac{1}{\sqrt{\beta\rho}} \tag{B.12}$$

This shows that the speed of sound in an arbitrary gas depends on the density, ρ, and the compressibility coefficient, β.

To calculate the speed of sound in air the compressibility coefficient of air must be known (the density is considered known for now). The compression process is not known in detail, but if the changes in pressure and volume are fast, the process can be assumed to be adiabatic (no heat transfer occurs) and it yields that

$$pV^{\gamma} = constant \tag{B.13}$$

where $\gamma = c_p/c_v$, c_p and c_v being the isobaric heat capacity and the isocoric heat capacity respectively. For an ideal diatomic gas it yields that $\gamma = 1.4$. According to [9] the diatomic assumption is a good approximation for air. The adiabatic assumption has been proved to give a very good agreement with experimental results and according to [11] this is also a good approximation. Differentiating (B.13) with respect to p gives

$$V^{\gamma} + \gamma p V^{\gamma-1}\frac{\partial V}{\partial p} = 0 \tag{B.14}$$

which is the same as

$$\frac{\partial V}{\partial p} = -\frac{V}{\gamma p} \tag{B.15}$$

It is now possible to calculate the compressibility coefficient by substituting (B.15) into (B.3)

$$\beta = -\frac{1}{V}\frac{\partial V}{\partial p} = -\frac{1}{V}(-\frac{V}{\gamma p}) = \frac{1}{\gamma p} \tag{B.16}$$

Finally, substituting this into (B.12) the speed of sound in a gas thus is

$$v = \sqrt{\frac{\gamma p}{\rho}} \tag{B.17}$$

depending on the pressure p, density ρ and the constant γ.